ANTIOXIDANTS & REDOX SIGNALING
Volume 22, Number 11, 2015

DOI: 10.1089/ars.2014.5969

ORIGINAL RESEARCH COMMUNICATION

Combined Sub-Optimal Doses of Rosuvastatin and Bexarotene Impair Angiotensin II-Induced Arterial Mononuclear Cell Adhesion Through Inhibition of Nox5 Signaling Pathways and Increased RXR/PPARα and RXR/PPARγ Interactions

Paula Escudero,[1,2] Aranzazu Martinez de Marañón,[1] Aida Collado,[1] Herminia Gonzalez-Navarro,[2] Carlos Hermenegildo,[2,3] Concepción Peiró,[4] Laura Piqueras,[2,*] and Maria-Jesus Sanz[1,2,*]

Abstract

Aim: Mononuclear cell (MC) infiltration into the arterial subendothelium is a key event in atherogenesis. Rosuvastatin (Rosu) and bexarotene (Bex) exert anti-inflammatory activity, but serious dose-related adverse effects have emerged. The need for safer and effective strategies to prevent and treat atherosclerosis led us to test the effect of combined use of both drugs on angiotensin II (Ang-II)-induced arterial MC recruitment. ***Results:*** Vehicle, Rosu (10–30 n*M*), Bex (0.3–1 μ*M*), or a combination of both were administered to human umbilical arterial endothelial cells (HUAECs) 20 h before stimulation with 1 μ*M* Ang-II (4 h). Surprisingly, a combination of Rosu (10 n*M*)+Bex (0.3 μ*M*), which did not influence Ang-II-induced MC recruitment when either stimulus was studied alone, significantly reduced this response. This effect was accompanied by diminished Ang-II-induced ICAM-1, VCAM-1, and CX_3CL1 endothelial expression and CXCL1, CXCL8, CCL2, and CCL5 production. Preincubation of HUAECs with Rosu+Bex inhibited Nox5 expression and Nox5-induced RhoA activation stimulated by Ang-II through increased RXRα, PPARα, and PPARγ expression in addition to RXRα/PPARα and RXRα/PPARγ interactions. *In vivo*, combined but not single administration of Rosu (1.25 mg/kg/day) and Bex (10 mg/kg/day) significantly diminished Ang-II-induced arteriolar leukocyte adhesion in the cremasteric microcirculation of C57BL/6 mice and atherosclerotic lesion formation in $apoE^{-/-}$ mice subjected to an atherogenic diet. ***Innovation and Conclusion:*** Combined administration of Bex+Rosu at suboptimal doses may constitute a new alternative and effective therapy in the control of the vascular inflammation associated to cardiometabolic disorders, since they synergize in their anti-inflammatory actions and may counteract their associated adverse effects. *Antioxid. Redox Signal*. 22, 901–920.

Introduction

Increased levels of circulating mediators, including angiotensin II (Ang-II) and cytokines, have been detected in cardiovascular and cardiometabolic diseases such as hypertension, obesity, and diabetes, and can exert deleterious effects on endothelial function (18, 34). These agents initiate an inflammatory signaling cascade associated with reactive oxygen species (ROS) generation, increased cell-surface expression of cell adhesion molecules (CAMs), and enhanced leukocyte adhesiveness to endothelial cells (18, 31). These responses are associated with endothelial dysfunction, and a pro-thrombotic and pro-inflammatory state of the endothelium (28) contributes to the early stages of atherogenesis (14, 28, 31).

[1]Department of Pharmacology, Faculty of Medicine, University of Valencia, Valencia, Spain.
[2]Institute of Health Research INCLIVA, University Clinic Hospital of Valencia, Valencia, Spain.
[3]Department of Pharmacology and Therapeutics, Faculty of Medicine, Universidad Autónoma de Madrid, Madrid, Spain.
[4]Department of Physiology, Faculty of Medicine, University of Valencia, Valencia, Spain.
*These authors contributed equally to this work.

Innovation

These findings highlight a promising new and safer therapeutic approach in the management of vascular inflammation that precedes or accompanies most cardiovascular disorders using two clinically available drugs. The synergistic anti-inflammatory effect was the consequence of increased RXRα, PPARα, and PPARγ expression as well as of RXRα/PPARα and RXRα/PPARγ interactions, leading to the inhibition of Nox5-mediated signaling pathways. Moreover, this new therapeutic regime results in minimal drug-associated side effects since low doses of both drugs are used, and rosuvastatin administration may beneficially counteract the dyslipidemic state linked to the chronic treatment with Bexarotene.

Ang-II is implicated in atherogenesis (9), and we demonstrated that 4 h of exposure to Ang-II *in vivo* caused arteriolar leukocyte adhesion in the mesenteric microcirculation of the rat (2). Notably, mononuclear leukocyte recruitment by Ang-II was found to be mediated largely by tumor necrosis factor-α (TNFα) and the subsequent increased endothelial expression of fractalkine (CX_3CL1)(37, 54). Consequently, pharmacological modulation of inflammatory cell infiltration of the subendothelial space may impede the atherogenic process associated with different cardiovascular risk factors related to the renninangiotensin system.

Statins are a group of 3-hydroxy-3-methylglutaryl coenzyme A reductase inhibitors that were primarily used because of their lipid-lowering properties due to their capacity to block cholesterol biosynthesis (1). Thereafter, their ability to reduce cardiovascular mortality and stroke was found to go beyond their lipid-lowering attributes. Indeed, when rosuvastatin (Rosu) was administered to healthy subjects without hyperlipidemia but with elevated high-sensitivity C-reactive protein levels, the incidence of major cardiovascular events was reduced (52). These so-called pleiotropic effects of statins include modulation of inflammatory reactions and anti-oxidant properties, which may additionally play important roles in statin-mediated cardiovascular protection (38). Accordingly, there is evidence indicating that statins favorably influence endothelial cell function (38) and impair leukocyte trafficking at sites of inflammation (59). Furthermore, a growing body of experimental data suggests a potential interplay between statins and peroxisome proliferator-activated receptors (PPARs) (3, 6), and activation of PPARs can downregulate the expression of CAMs, proinflammatory genes, and leukocyte-endothelial cell interactions (40). Though statins in general are well tolerated, myopathy and acute renal events have been a significant concern with the use of high-potency statin drugs, in particular simvastatin and Rosu (8, 15, 23). Since these adverse effects are frequently dose related (8, 15, 23), there remains an overt need to identify agents that, when combined with statins, can provide the greatest benefit on cardiovascular disease with the least added risk.

Bexarotene (Bex) is a retinoid X receptor (RXR)-selective agonist currently used in the treatment of cutaneous T-cell lymphoma. We have previously shown that Bex can inhibit mononuclear leukocyte attachment to stimulated arterial endothelial cells through downregulation of redox-sensitive pathways and *via* RXR/PPARγ interaction (12, 55). Indeed, it is well established that PPARs form permissive RXR heterodimers that synergistically respond to agonists of RXR and the partner receptor (49). Unfortunately, Bex treatment is associated with unavoidable and dose-limiting side effects, in particular hypertriglyceridemia, hypercholesterolemia, and, to a lesser extent, hypothyroidism (7, 61). However, Rosu administration can reduce triglyceride levels (13) and the U.K. consensus statement on safe clinical prescribing of Bex recommend the use of this statin to prevent the dyslipidemic effects associated with administration of the RXR agonist (57).

In an attempt to identify more effective strategies to treat and prevent atherosclerosis, coronary heart disease, and comorbid metabolic disorders characterized by endothelial dysfunction, we have evaluated the effect of combined treatment with Rosu and Bex. In this study, we provide both *in vitro* and *in vivo* evidence that the combination of Rosu + Bex at suboptimal concentration/doses provokes a clear impairment in Ang-II-induced mononuclear cell (MC) adhesion to the arterial endothelium. The underlying mechanisms involved in this beneficial synergism were also explored. We found that Nox5 downregulation and subsequent RhoA inactivation were involved in these responses. Furthermore, increased RXR/$PPAR_\alpha$ and RXR/PPARγ interactions were, in part, responsible for the observed anti-inflammatory activity.

Results

A combination of Rosu and Bex at suboptimal concentrations reduces Ang-II-induced human umbilical artery endothelial cell MC adhesion

Initially, we evaluated the effect of Ang-II challenge on mononuclear leukocyte-endothelial cell interactions *in vitro* using the dynamic flow chamber assay. Thus, freshly isolated human MCs were perfused across human umbilical artery endothelial cell (HUAEC) monolayers stimulated or not with Ang-II (1 μM) for 4 h. Ang-II caused a significant increase in mononuclear leukocyte adhesion to arterial endothelial cells (Fig. 1). To assess the effect of Rosu on Ang-II-induced MC recruitment, HUAECs were pretreated with the statin at two different concentrations (10 and 30 nM), 20 h before Ang-II stimulation. While 10 nM Rosu had no impact on Ang-II-induced MC recruitment, preincubation with 30 nM Rosu significantly reduced Ang-II-induced mononuclear leukocyte adhesion (Fig. 1A). A similar approach was followed to test the effect of Bex preincubation on Ang-II-induced responses, based on previous observations (55). As anticipated, 1 μM but not 0.3 μM Bex significantly inhibited MC adhesion to Ang-II-stimulated HUAECs (Fig. 1B). To evaluate the potential synergism of both drugs, different combinations of Rosu and Bex were assessed. All the combinations tested significantly impaired Ang-II-induced MC attachment to the arterial endothelium (Fig. 1C). Unexpectedly, the combination of Rosu at 10 nM and Bex at 0.3 μM, which displayed no significant effect when either treatment was tested alone, reduced adhesion by 51% (Fig. 1C). Consequently, in all subsequent *in vitro* experiments, this combination of Rosu and Bex (designated Rosu + Bex) was employed to explore the underlying mechanisms involved in this response.

In addition, since there is evidence to support that Ang-II can decrease AT_1 receptor expression, although in vascular smooth muscle cells (44), we evaluated this possibility. As illustrated in Supplementary Figure S1 (Supplementary Data

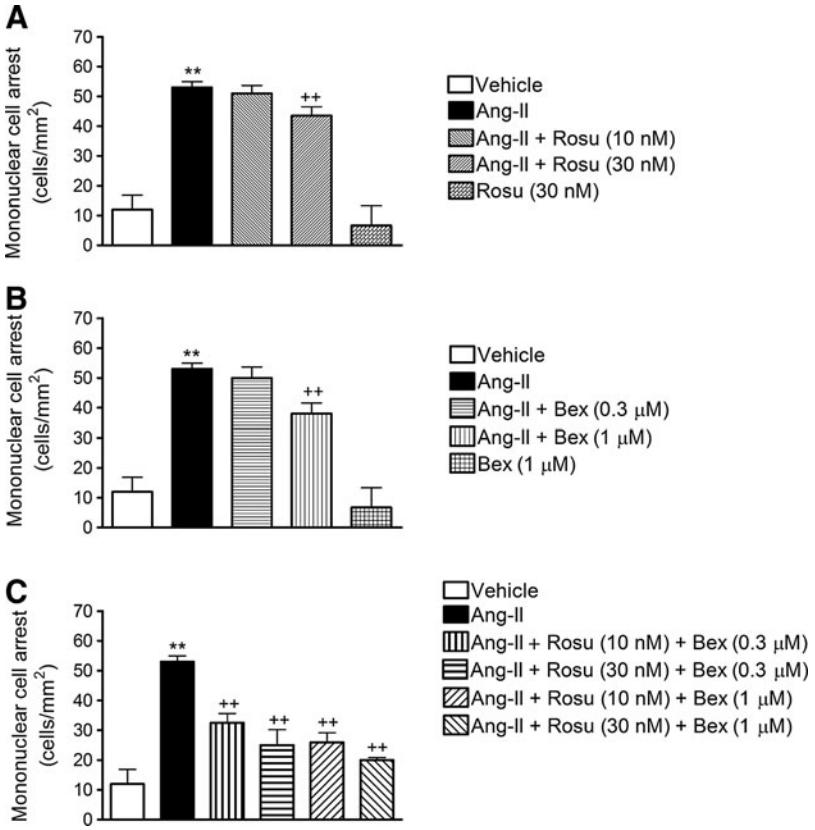

FIG. 1. Combination of Rosuvastatin (Rosu) and Bexarotene (Bex) at suboptimal concentrations reduces angiotensin II (Ang-II)-induced human umbilical artery endothelial cell (HUAEC) mononuclear cell adhesion under physiological flow. HUAECs were stimulated with Ang-II (1 μM) for 4 h. In some experiments, cells were pretreated with Rosu (10–30 nM) **(A)**, Bex (0.3–1 μM) **(B),** or combinations of both **(C)**, 20 h before Ang-II stimulation. Freshly isolated human mononuclear cells (10^6 cells/ml) were perfused across the endothelial monolayers for 5 min at 0.5 dyn/cm^2, and leukocyte adhesion was quantified. Results are the mean ± SEM of $n = 5$ independent experiments; $^{**}p < 0.01$ relative to the vehicle group, $^{++}p < 0.01$ relative to the Ang-II-stimulated cells.

are available online at www.liebertpub.com/ars), we found that neither Ang-II stimulation for 4 h nor the pretreatment of the endothelial cells with the drugs, in combination or alone, affected AT_1 receptor expression.

Decreased expression of ICAM-1 and VCAM-1 is involved in the reduced Ang-II-induced HUAEC-MC adhesion caused by suboptimal concentrations of Rosu+Bex

To investigate whether the inhibitory effects exerted by Rosu+Bex on Ang-II-induced mononuclear leukocyte adhesion were mediated through modulation of endothelial CAM expression, intercellular adhesion molecule-1 (ICAM-1) and vascular cell adhesion molecule-1 (VCAM-1) protein expression were determined by flow cytometry and immunocytochemistry. Stimulation with Ang-II resulted in a significant upregulation of ICAM-1 and VCAM-1 expression when compared with unstimulated control HUAECs, as measured by both flow cytometry and immunofluorscence (Fig. 2A, B). Pretreatment of cells with Rosu or Bex did not modify the increased endothelial CAM expression induced by the peptide (Fig. 2A, B). In contrast, preincubation of HUAEC with Rosu+Bex resulted in a significant decrease in Ang-II-induced ICAM-1 and VCAM-1 expression, by 42% and 66%, respectively (Fig. 2A, B).

Inhibition of Ang-II-induced HUAEC chemokine synthesis by combination of Rosu+Bex at suboptimal concentrations

Since Ang-II stimulation of endothelial cells can induce the production and release of different CXC and CC chemokines, in addition to the expression of the membrane-bound chemokine fractalkine (36, 42, 54), we next evaluated the effect of Rosu+Bex on Ang-II-induced chemokine synthesis in human arterial endothelial cells. Significant increases in the levels of growth-regulated oncogene-α (GROα or CXCL1), interleukin-8 (IL-8 or CXCL8), monocyte chemotactic protein-1 (MCP-1 or CCL2), and regulated on activation, normal T cell expressed and secreted (RANTES or CCL5) were detected in the supernatant of HUAEC subjected to Ang-II stimulation for 4 h, as measured by enzyme-linked immunoassay (ELISA) (Fig. 3A–D). This increase was not inhibited when HUAECs were preincubated with either of the drugs alone, but was markedly diminished by pretreatment of cells with the combination of Rosu+Bex (Fig. 3A–D). Similarly, when HUAECs were stimulated with 1 μM Ang-II for 24 h, a significant increase in the expression of fractalkine was observed, by both flow cytometry and immunofluorescence (Fig. 3E, F). Again, preincubation of cells with Rosu+Bex caused a significant downregulation of the cell-membrane chemokine expression (Fig. 3E, F).

Combination of Rosu+Bex at suboptimal concentrations inhibits Ang-II-induced HUAEC RhoA activation and subsequent MC recruitment

It is well recognized that small GTP-binding proteins (G-proteins), such as Ras, Rho, and Rac, are activated by Ang-II through interaction with its AT_1 receptor (22). To characterize the signaling mechanisms by which Rosu+Bex modulate arterial MC adhesion stimulated by Ang-II, we first established their effect on Ang-II-induced RhoA activation. As illustrated in Figure 4A, Ang-II stimulation of HUAEC for

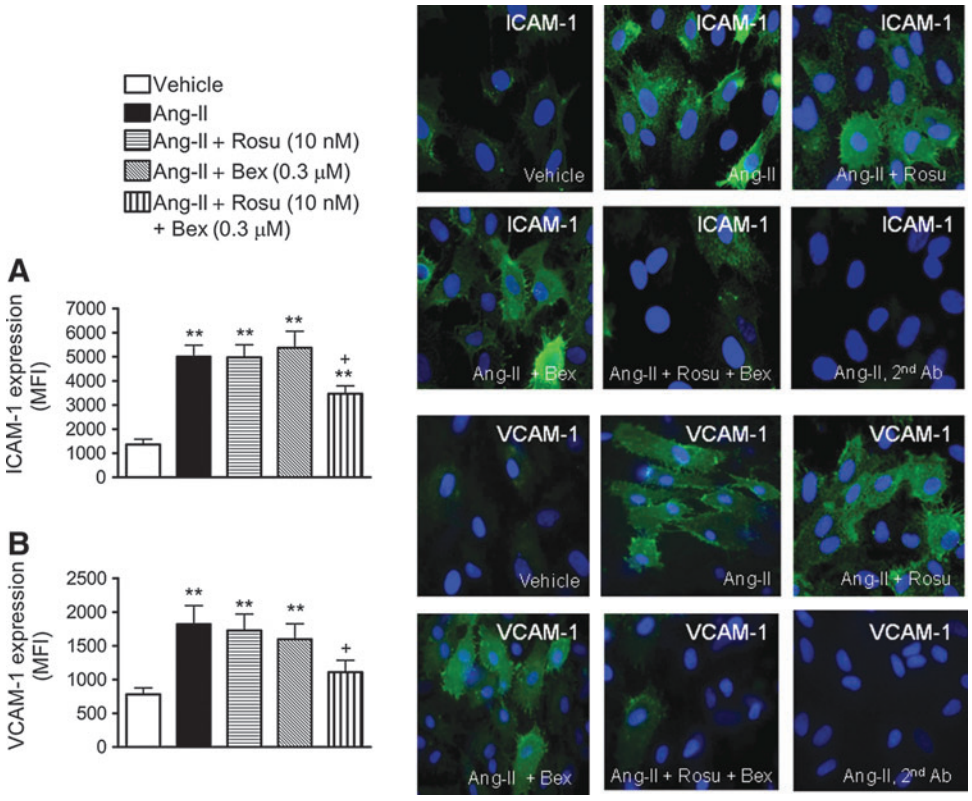

FIG. 2. Effect of Rosu+Bex on endothelial cell adhesion molecule expression. Cells were treated with Rosu (10 n*M*), Bex (0.3 μM), or a combination of Rosu (10 n*M*) plus Bex (0.3 μM) for 20 h and then stimulated with Ang-II (1 μM, 4 h). ICAM-1 **(A)** and VCAM-1 **(B)** protein expression was determined by flow cytometry and immunofluorescence. *Right panels* show representative images of endothelial cells. Nuclei were counterstained with DAPI (*blue*), and *green* fluorescence shows ICAM-1 (*top*) or VCAM-1 (*bottom*). Results are expressed as mean ± SEM of $n = 5$–9 independent experiments; $^{**}p < 0.01$ relative to the vehicle group, $^{+}p < 0.05$ relative to the Ang-II-stimulated cells.

1 h caused a significant increase in RhoA activation. Whereas pretreatment of cells with Rosu or Bex 20 h before Ang-II stimulation failed to modify RhoA activation, preincubation with the combination Rosu + Bex caused a significant inhibition of this response (Fig. 4A). To evaluate the impact of RhoA activation on Ang-II-induced MC recruitment, we silenced RhoA expression in endothelial cells with small interfering RNA (siRNA). Forty–eight hours after transfection with RhoA–specific siRNA, HUAEC exhibited a >69% reduction in RhoA protein compared with control siRNA-treated cells (Fig. 4B). Ang-II stimulation (1 μM, 4 h) produced a significant increase in MC arrest in control siRNA cells, which was abrogated in RhoA-silenced HUAECs (Fig. 4C). Furthermore, inhibition of the RhoA downstream target, Rho-associated protein kinase (ROCK), resulted in a significant impairment in Ang-II-induced arterial mononuclear leukocyte adhesion (Supplementary Fig. S2).

Combination of Rosu+ Bex at suboptimal concentrations inhibits Ang-II-induced Nox5 expression in HUAECs

The production of ROS and subsequent activation of redox-sensitive signaling pathways mediates many of the inflammatory responses induced by Ang II (29, 30). Accordingly, endothelial Ang-II stimulation activated NADPH oxidase in HUAECs (Fig. 5A). Notably, this activation was diminished by cell pretreatment with Rosu + Bex, but not when either drug was used separately (Fig. 5A). Ang-II caused increased endothelial expression of Nox2, Nox4, and Nox5 (54) and Figure 5B–D. Interestingly, while the expression of these Nox isoforms induced by Ang-II were unaffected by Rosu or Bex pretreatment of the cells, Nox2 and Nox5 but not Nox4 expression was markedly reduced by preincubation with Rosu + Bex (Fig. 5B–D). Since MC arrest was found to be largely mediated *via* endothelial Nox5 expression (54) and ROS generation can activate RhoA (43), we next questioned whether the absence of endothelial Nox5 or antioxidant pretreatment resulted in a failure to activate this GTP-binding protein. To do this, we used both siRNA targeting Nox5 and the antioxidant apocynin. Nox5 protein expression was significantly reduced (62%) after 48 h of incubation with a specific siRNA (Supplementary Figs. S3 and S4). Further, knockdown of Nox5 or apocynin pretreatment resulted in the blockade of Ang-II-induced RhoA activation (Fig. 5E, F). Conversely, in RhoA-silenced HUAECs, or in HUAECs pretreated with an RhoA inhibitor (cell-permeable C3 transferase), the increased expression of Nox5 protein triggered by Ang-II remained unchanged (Fig. 5G, H). Moreover, while Ang-II-induced endothelial ROS generation was neutralized by preincubation with apocynin, it was unaffected by pretreatment of the cells with the RhoA inhibitor (Supplementary Fig. S5).

Suboptimal concentrations of Rosu+ Bex provokes increased expression of endothelial RXRα, PPARα, and PPARγ

Given that statins and Bex can activate PPARs and RXRα nuclear receptors, respectively (3, 6, 55), we investigated whether the combination of Rosu + Bex exerted its inhibitory activity through changes in the endothelial expression of RXRα, PPARα, PPARβ/δ, or PPARγ. Immunoblot analysis showed that Ang-II-stimulated HUAECs, preincubated or not with Ros or Bex alone, expressed comparable levels of RXRα and PPAR nuclear receptors to vehicle controls (Fig. 6A–D). Importantly, when cells were treated with Rosu + Bex for

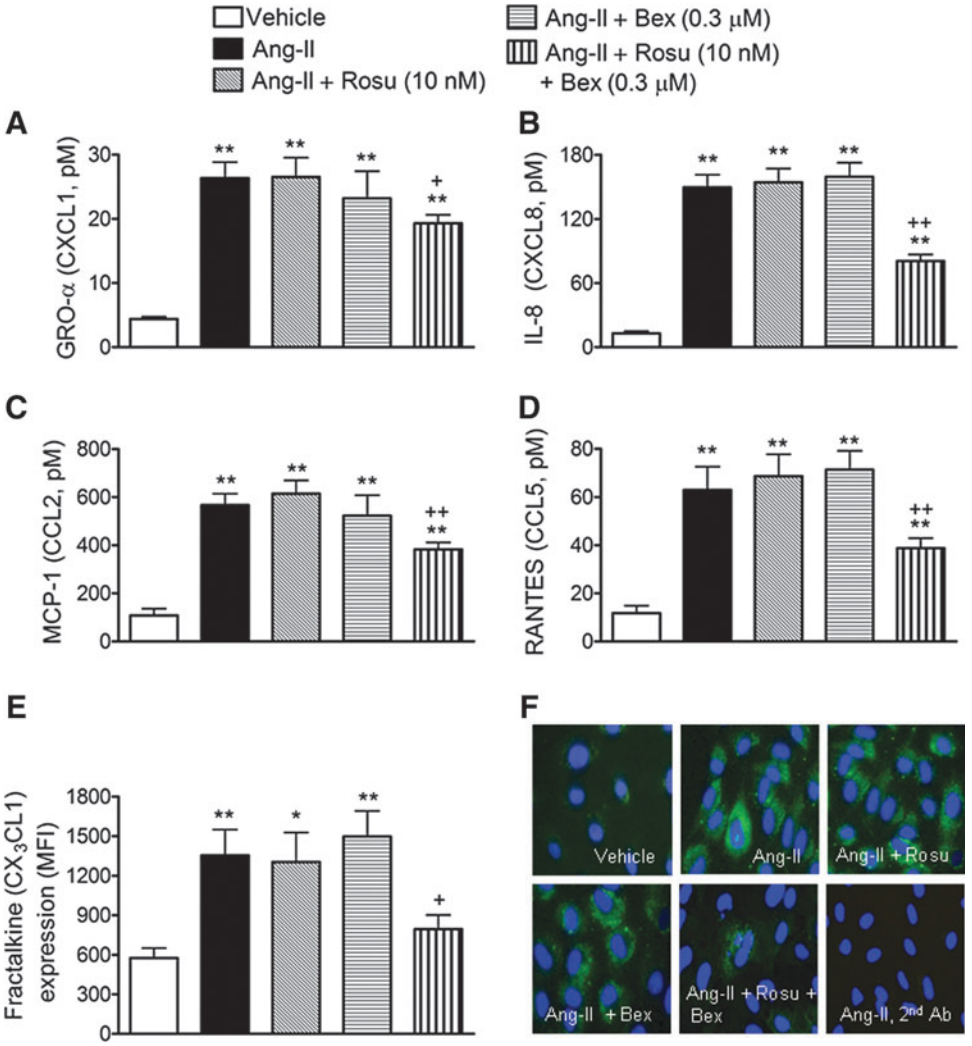

FIG. 3. Suboptimal concentrations of Rosu+Bex decreases Ang-II-induced chemokine production in HUAEC. Cells were treated with Rosu (10 n*M*), Bex (0.3 μM), or a combination of Rosu (10 n*M*) plus Bex (0.3 μM) for 20 h and then stimulated with Ang-II (1 μM) for 4 h. GROα **(A)**, IL-8 **(B)**, MCP-1**(C),** and RANTES **(D)** release was determined by enzyme-linked immunoassay (ELISA) in the cell-free supernatant. Results are expressed as pM concentration and presented as mean ± SEM of $n = 7$–9 independent experiments; $^{**}p < 0.01$ relative to the vehicle group, $+p < 0.05$ or $++p < 0.01$ relative to the Ang-II stimulated cells. In a second set of experiments, HUAECs were treated with Rosu (10 n*M*), Bex (0.3 μM), or a combination of Rosu (10 n*M*) plus Bex (0.3 μM) for 20 h and then stimulated with Ang-II (1 μM) for 24 h. CX_3CL1 expression in HUAEC was determined by flow cytometry **(E)** and visualized by immunofluorescence (*green*). Nuclei were counterstained with DAPI; images are representatives of $n = 5$–7 independent experiments per group **(F)**. Results are the mean ± SEM of $n = 5$–7 independent experiments; $^{*}p < 0.05$ or $^{**}p < 0.01$ relative to the vehicle group, $+p < 0.05$ relative to the Ang-II-stimulated cells.

20 h followed by stimulation with Ang-II for 4 h, RXRα, PPARα, and PPARγ were significantly upregulated while PPARβ/δ expression was unchanged (Fig. 6A–D). To understand how increased expression of RXRα, PPARα, or PPARγ might contribute to the reduction of Ang-II-induced leukocyte-endothelial cell interactions elicited by pre-exposure of HUAEC to Rosu + Bex, we evaluated leukocyte adhesion to HUAECs individually silenced for expression of RXRα, PPARα, and PPARγ. Knockdown of RXRα, PPARα, and PPARγ resulted in a 57–66% decrease in receptor expression relative to control-siRNA cells (Supplementary Fig. S6). Notably, silencing of RXRα, PPARα, or PPARγ abolished the suppressive effects of Rosu + Bex on leukocyte adhesion to HUAEC stimulated with Ang-II (Fig. 6E–G). Furthermore, when HUAEC were immunoprecipitated with an anti-PPARα or an anti-PPARγ antibody, followed by immunoblotting with an anti-RXRα antibody, enhanced dimerization of RXRα with PPARα or PPARγ was detected with Rosu + Bex, relative to Ang-II-only stimulated cells (Fig. 6H), although the interaction seemed to be more pronounced with PPARγ.

Reduction of RXRα, PPARα, or PPARγ expression blunted the inhibition of Ang-II-induced HUAEC RhoA activation and Nox5 expression by Rosu + Bex at suboptimal concentrations

To gain further insight into the inhibitory mechanisms involved in the Ang-II-induced MC arrest by Rosu + Bex,

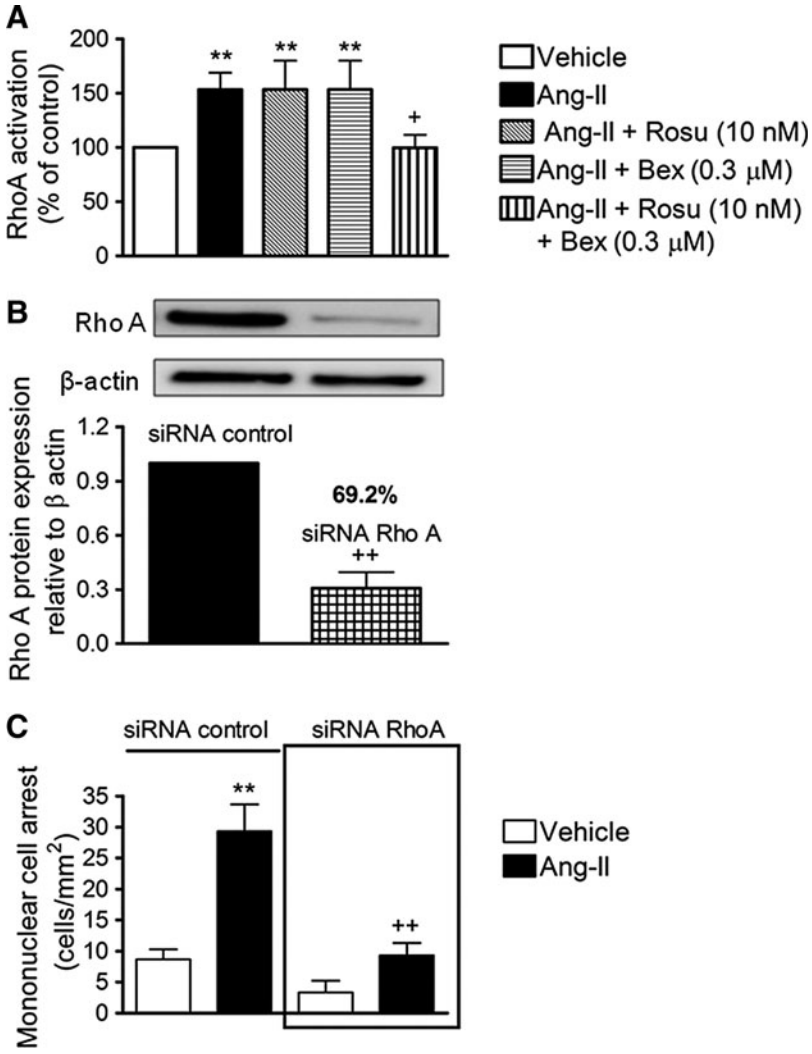

FIG. 4. Inhibitory effects of Rosu+Bex at suboptimal concentrations on Ang-II-induced HUAEC RhoA activation. HUAEC were stimulated with Ang-II (1 μM) for 1 h. In some experiments, cells were treated with Rosu (10 nM), Bex (0.3 μM), or a combination of Rosu (10 nM) plus Bex (0.3 μM) for 20 h before Ang-II stimulation. Quantification of RhoA-GTP activity was determined using a colorimetric G-Lisa kit activation RhoA assay **(A)**. Results are the mean ± SEM of $n = 6$–9 independent experiments and presented as percentage of control; $^{**}p < 0.01$ relative to the vehicle group, $^{+}p < 0.05$ relative to the Ang-II-stimulated cells. A second group of cells was transfected using an RhoA-specific siRNA or control-siRNA, and at 48 h post-transfection protein, expression was determined by immunoblot **(B)**. Control or RhoA-specific siRNA-transfected cells were stimulated with Ang-II (1 μM) for 4 h. Then, freshly isolated human mononuclear cells were perfused over the endothelial monolayers for 5 min at 0.5 dyn/cm^2 and leukocyte adhesion was quantified **(C)**. Results are the mean ± SEM of $n = 5$–6 independent experiments; $^{**}p < 0.01$ relative to the vehicle group, $^{++}p < 0.01$ relative to values in Ang-II group in control siRNA-transfected cells.

FIG. 5. Suboptimal concentrations of Rosu+Bex decrease Ang-II-induced endothelial Nox5 expression. Endothelial cells were incubated with Rosu (10 nM), Bex (0.3 μM), or a combination of Rosu (10 nM) plus Bex (0.3 μM) for 20 h and then stimulated with Ang-II (1 μM, 1 h) and the generation of superoxide anions by NADPH oxidase was determined by lucigenin-derived chemiluminiscence **(A)**. Results (mean ± SEM of four to seven independent experiments performed in duplicate) are presented as percentage of control; $^{**}p < 0.01$ relative to the vehicle group, $^{+}p < 0.05$ relative to the Ang-II-stimulated cells. HUAEC were treated with Rosu (10 nM), Bex (0.3 μM), or a combination of Rosu (10 nM) plus Bex (0.3 μM) for 20 h and then stimulated with Ang-II (1 μM, 24 h). Nox2 **(B)**, Nox4 **(C),** and Nox5 **(D)** expression was determined by immunoblotting. Results (mean ± SEM of five to seven independent experiments) are expressed as fold increase of Nox:β-actin. Representative blots are shown; $^{*}p < 0.05$ or $^{**}p < 0.01$ relative to the vehicle group, $^{+}p < 0.05$ or $^{++}p < 0.01$ relative to the Ang-II stimulated cells. In additional experiments, control or siRNA Nox5-transfected HUAEC were stimulated with Ang-II (1 μM for 1 h) and quantification of RhoA-GTP activity was determined as earlier **(E)**. Results are the mean ± SEM of $n = 7$–8 independent experiments and are presented as percentage of control siRNA-transfected cells, $^{**}p < 0.01$ relative to the respective vehicle group, $^{+}p < 0.05$ relative to the respective Ang-II-stimulated cells. In other plates, HUAEC were pretreated with the NADPH inhibitor apocynin (30 μM) 1 h before Ang-II stimulation and quantification of RhoA activity was determined **(F)**. Results are the mean ± SEM of $n = 5$ independent experiments and presented as percentage of control; $^{**}p < 0.01$ relative to the vehicle-treated group, $^{+}p < 0.05$ relative to the Ang-II-stimulated cells. In a different experimental setting, cells were transfected with control or RhoA-specific siRNA. At 48 h post transfection, HUAEC were stimulated with Ang-II (1 μM) for 4 h and Nox5 expression was quantified by immunoblot **(G)**. Results (mean ± SEM of at least five independent experiments) are expressed as fold increase of Nox5:β-actin of control siRNA-transfected cells. A representative blot is shown above; $^{**}p < 0.01$ relative to the vehicle-treated group. Untransfected cells were pretreated with an RhoA inhibitor (C3 transferase, 2 μg/ml for 4 h) before Ang-II stimulation, and Nox5 expression was determined by immunoblot. **(H)** Results (mean ± SEM of at least five independent experiments) are expressed as fold increase of Nox5:β-actin. A representative blot is shown above; $^{**}p < 0.01$ relative to the vehicle-treated group.

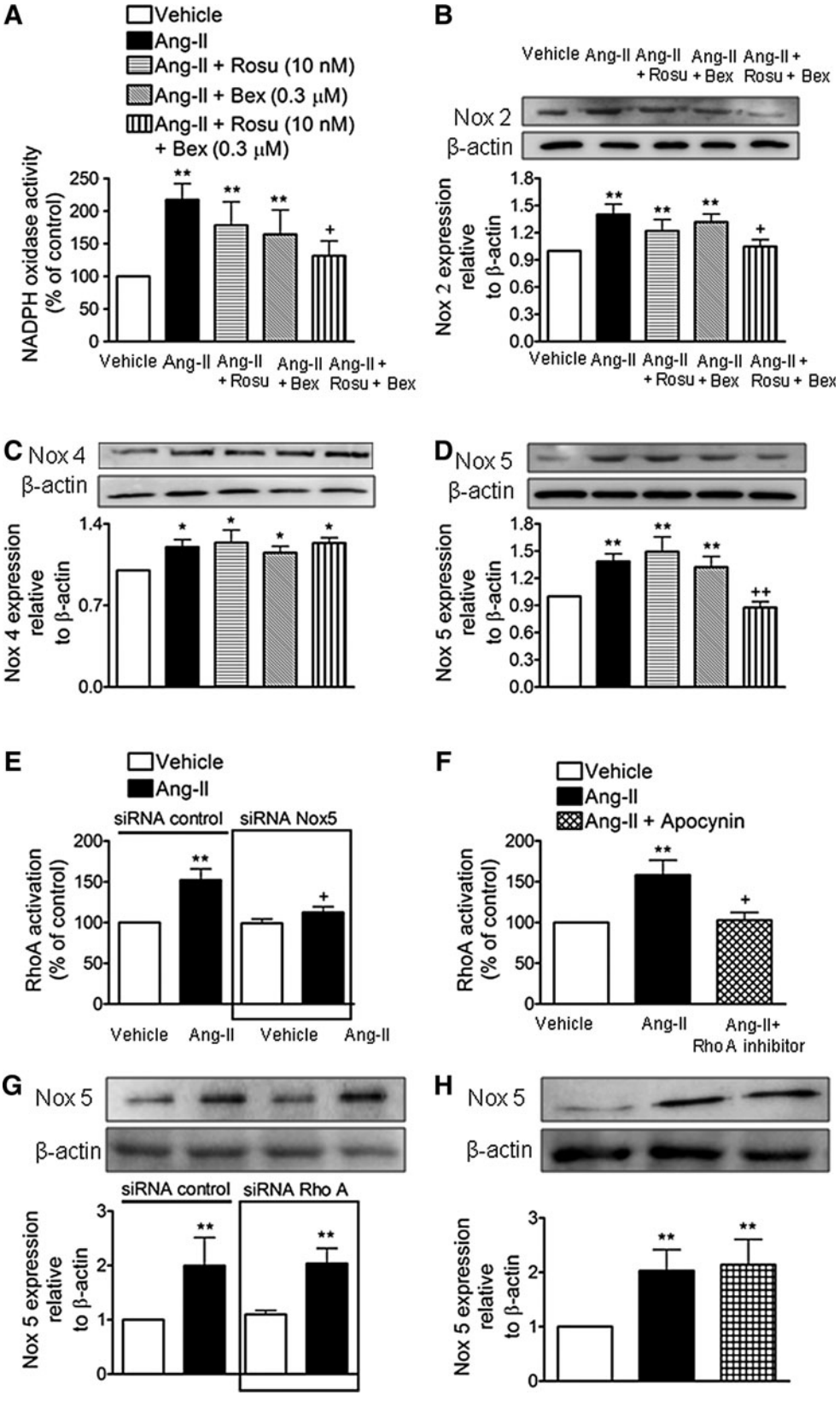
A
Vehicle
Ang-II
Ang-II + Rosu (10 nM)
Ang-II + Bex (0.3 μM)
Ang-II + Rosu (10 nM) + Bex (0.3 μM)
NADPH oxidase activity (% of control)
Vehicle
Ang-II
Ang-II + Rosu
Ang-II + Bex
Ang-II + Rosu + Bex
B
Nox 2
β-actin
Nox 2 expression relative to β-actin
C
Nox 4
β-actin
Nox 4 expression relative to β-actin
D
Nox 5
β-actin
Nox 5 expression relative to β-actin
E
siRNA control
siRNA Nox5
RhoA activation (% of control)
F
Ang-II + Apocynin
Ang-II + RhoA inhibitor
G
siRNA Rho A
H

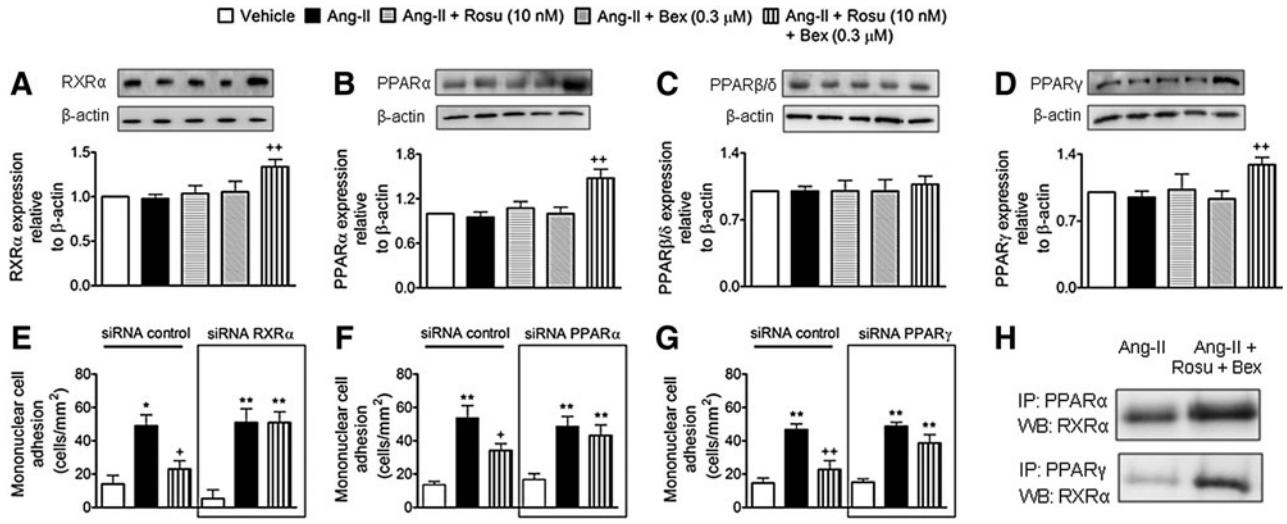

FIG. 6. Suboptimal concentrations of Rosu+Bex increase RXRα, PPARα, and PPARγ but not PPARβ/δ expression in HUAEC stimulated with Ang-II. RXRα, PPARα, or PPARγ knockdown abolished the inhibitory effect of Rosu + Bex on Ang-II-induced mononuclear leukocyte-endothelial cell interactions. HUAEC were incubated with Ang-II (1 μM) for 4 h. In some experiments, cells were pretreated with Rosu (10 nM), Bex (0.3 μM), or a combination of Rosu (10 nM) plus Bex (0.3 μM) for 20 h before Ang-II stimulation. RXRα **(A)**, PPARα **(B)**, PPARγ **(C),** and PPARβ/δ **(D)** expression was determined by immunoblot. Results (mean ± SEM of $n = 5$–7 independent experiments) are expressed as fold increase relative to β-actin. Representative gels are shown. $^{++}p < 0.01$ relative to the Ang-II-treated group. Cells were transfected with control siRNA, RXRα-specific siRNA **(E)**, PPARα-specific siRNA **(F),** or PPARγ-specific siRNA **(G)** and stimulated with Ang-II (1 μM; 4 h) at 48 h post-transfection. In some experiments, cells were pretreated with Rosu (10 nM) plus Bex (0.3 μM) 20 h before Ang-II challenge. Freshly isolated human mononuclear cells (10^6 cells/ml) were perfused over the endothelial monolayers for 5 min at 0.5 dyn/cm^2, and leukocyte adhesion was quantified. Results are the mean ± SEM of $n = 4$–5 independent experiments. $^{*}p < 0.05$ or $^{**}p < 0.01$ relative to the respective vehicle group, $^{+}p < 0.05$ or $^{++}p < 0.01$ relative to the respective Ang-II-stimulated cells. RXRα/PPARα and RXRα/PPARγ interactions **(H)** were assessed by immunoprecipitation of PPARα or PPARγ and subsequent immunoblotting for RXRα. Blots are representative of four independent experiments.

HUAEC were transfected with siRNAs against RXRα, PPARα, or PPARγ. Interestingly, the inhibitory effect of Rosu + Bex on RhoA activation or Nox5 downregulation in cells stimulated with Ang-II was abolished in cells silenced for these nuclear receptors (Fig. 7).

Combination of Rosu+Bex at suboptimal concentrations restored the inhibition in nitric oxide bioavailability induced by Ang-II in HUAECs

It is well known that Ang-II impairs endothelial function by decreasing nitric oxide (NO) bioavailability (32, 43). These effects can be mediated through superoxide anion generation and a reaction with NO, resulting in its quenching to form peroxynitrite, and endothelial NO synthase (eNOS) inhibition and uncoupling (32, 43). Therefore, we evaluated the effect of Rosu + Bex on the Ang-II-induced decrease in NO bioavailability in HUAEC. Ang-II stimulation of the cells reduced NO levels in HUAECs (Fig. 8A). Notably, this reduction was reversed by cell pretreatment with Rosu + Bex, but not when either drug was used separately (Fig. 8A). Pretreatment of the cells with the antioxidant apocynin or an RhoA inhibitor (cell permeable C3 transferase) reversed the reduction in NO availability induced by Ang-II (Fig. 8B). Similarly, silencing of Nox5 prevented the decrease in NO bioavailability provoked by Ang-II (Fig. 8C). More importantly, in the absence of RXRα, PPARα, or PPARγ, Rosu + Bex was unable to fully restore endothelial NO levels (Fig. 8D–G).

Suboptimal doses of Rosu+Bex impairs Ang-II-induced leukocyte-arteriolar adhesion in vivo

To connect our *in vitro* observations with what happens *in vivo*, we utilized a chronic model of Ang-II infusion. Animals were implanted with osmotic mini-pumps constantly releasing either Ang-II (500 ng/kg/min) (56) or vehicle, for 14 days. Consistent with the *in vitro* analysis, animals chronically infused with Ang-II showed a significant enhancement in arteriolar leukocyte adhesion compared with vehicle-infused mice (Fig. 9A). Co-infusion of Rosu at 1.25 mg/kg/day, or oral administration of Bex at 10 mg/kg/day, did not change arteriolar leukocyte adhesion caused by Ang-II systemic infusion (Fig. 9A). However, when the animals were co-infused with Ang-II plus the statin, and Bex was co-administered daily, leukocyte adhesion was significantly reduced by 65% (Fig. 9A). Moreover, Ang-II-induced expression of CD11b in circulating monocytes was also reduced by Rosu + Bex administration, whereas neutrophil CD11b expression was not affected by any treatment (Fig. 9B, C). In addition, immunohistochemistry analysis of cremasteric arterioles showed that the Ang-II-induced increase in ICAM-1, VCAM-1, and fractalkine expression was blunted by co-treatment with Rosu + Bex in mice (Fig. 9D). As expected, a significant reduction in circulating levels of chemokines, including CXCL1 and MCP-1, and a tendency for reduction in RANTES, were also observed in animals treated with Rosu + Bex and chronically subjected to Ang-II (Fig. 9E–G). In this

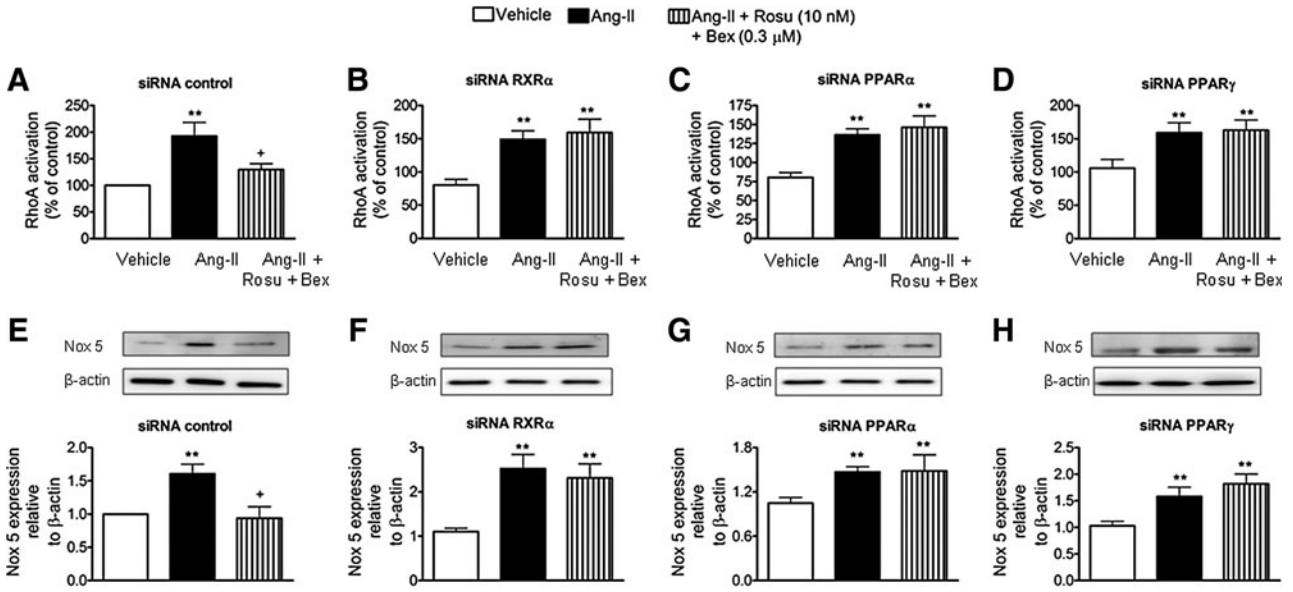

FIG. 7. Silencing of endothelial RXRα, PPARα, or PPARγ blunted the inhibition of Ang-II-induced HUAEC RhoA activation and Nox5 expression by the combination of Rosu + Bex at suboptimal concentrations. Cells were transfected with control siRNA **(A)**, RXRα-specific siRNA **(B)**, PPARα-specific siRNA **(C),** or PPARγ-specific siRNA **(D)** and stimulated with Ang-II (1 μM; 1 h) at 47 h post-transfection. In some experiments, cells were pretreated with Rosu (10 nM) plus Bex (0.3 μM) 20 h before Ang-II challenge. Quantification of RhoA-GTP activity was determined using a colorimetric G-Lisa RhoA activation assay. Results are the mean ± SEM of $n = 5$–7 independent experiments and presented as percentage of control siRNA-transfected cells; $^{**}p < 0.01$ relative to the respective vehicle group, $^{+}p < 0.05$ relative to the respective Ang-II stimulated cells. Following a similar protocol but after stimulation with 1 μM Ang-II for 24 h at 24 h post-transfection, Nox5 expression **(E–H)** was determined by immunoblotting. Results (mean ± SEM of five to six independent experiments) are expressed as fold increase of Nox5:β-actin of control siRNA-transfected cells. Representative blots are shown; $^{**}p < 0.01$ relative to the respective vehicle group, $^{+}p < 0.05$ relative to the respective Ang-II-stimulated cells.

experimental setting, glucose levels and lipid profile were unaffected by the different treatments (Supplementary Table S1). With regard to blood pressure, Ang-II infusion at this dose caused a small but significant increase in this parameter at day 14, which was more marked when the peptide was infused at 1000 ng/kg/min (Supplementary Table S2). However, none of the treatments applied affected the increase in blood pressure induced by Ang-II (Supplementary Table S2).

In an additional group of experiments using murine aortic endothelial cells, increased Nox2 and Nox4, but not dual oxidase 1 and 2 (Duox1 and Duox2), mRNA expression was detected in Ang-II-stimulated cells (Supplementary Fig. S7). Interestingly, whereas Nox2 expression was impaired by cell pretreatment with Rosu + Bex, Nox4 expression was unaffected by the combination treatment (Supplementary Fig. S7). In accordance with the results from human cells, neither drug affected Ang-II-induced Nox2 or Nox4 expression when evaluated separately (Supplementary Fig. S7).

Suboptimal doses of Rosu+ Bex reduce atherosclerosis development and cell composition in apoE$^{-/-}$ mice on atherogenic diet

To explore the potential relevance of these findings for atherosclerosis, 8-week-old apoE$^{-/-}$ mice were fed a high-fat atherogenic diet for 8 weeks. As expected, animals subjected to an atherogenic diet presented increased lesion formation and infiltration of macrophages and T cells within the lesion (Fig. 10). Co-infusion of Rosu at 1.25 mg/kg/day, or oral administration of Bex at 10 mg/kg/day, had no effect on these parameters (Fig. 10). Notably, chronic treatment with the statin plus Bex substantially decreased lesion formation and the associated MC infiltration (Fig. 10). Neither glucose level nor the lipid profile in atherogenic animals was significantly affected by the different treatments applied (Supplementary Table S3).

Discussion

Combination therapy that simultaneously addresses multiple mechanisms involved in the pathogenesis of atherosclerosis is an attractive emerging concept for preventing and/or slowing the progression of this disease. Using both *in vitro* and *in vivo* approaches, we provide the first demonstration of an anti-inflammatory effect of suboptimal concentrations/doses of two commercially available drugs, Rosu and Bex, in combination.

Mononuclear leukocyte infiltration into the subendothelial space is a key event in the atherogenic process (31) and treatment with Rosu or Bex has been shown to limit MC numbers in atherosclerotic plaques, or their interaction with the arterial endothelium (27, 55). In this study, stimulation of arterial endothelial cells with Ang-II, mimicking a dysfunctional endothelium, promoted the adhesion of mononuclear leukocytes, and this event was clearly reduced by different combined treatments of Rosu and Bex. Remarkably, this reduction was achieved with a suboptimal combination of Rosu (10 nM) and Bex (0.3 μM) since at these concentrations, neither the statin nor the RXR ligand displayed any

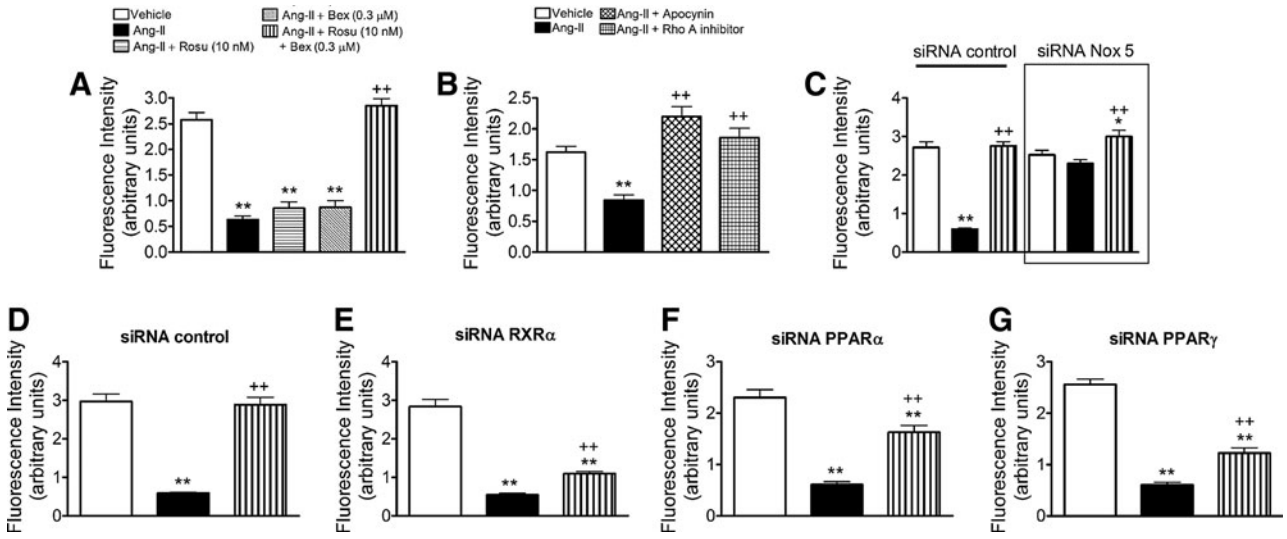

FIG. 8. Combination of Rosu+Bex at suboptimal concentrations reversed the inhibition in nitric oxide (NO) bioavailability induced by Ang-II in HUAECs. Endothelial cells were incubated with Rosu (10 n*M*), Bex (0.3 μM), or a combination of Rosu (10 n*M*) plus Bex (0.3 μM) for 20 h and then stimulated with Ang-II (1 μM, 4 h), and intracellular NO was monitored with (DAF-2-FM diacetate) **(A)**. Results (mean ± SEM of at least five independent experiments performed in triplicate); $^{**}p < 0.01$ relative to the vehicle group, $^{++}p < 0.01$ relative to the Ang-II treated group. In additional experiments, endothelial cells were pretreated with the antioxidant apocynin (30 μM for 1 h) or with an RhoA inhibitor (C3 transferase, 2 μg/ml for 4 h) before Ang-II stimulation (1 μM, 1 h). Intracellular NO was monitored with (DAF-2-FM diacetate) **(B)**. Results (mean ± SEM of at least five independent experiments performed in triplicate); $^{**}p < 0.01$ relative to the vehicle group, $^{++}p < 0.01$ relative to the Ang-II-treated group. Control or siRNA Nox5-transfected HUAEC were stimulated with Ang-II (1 μM for 4 h), and quantification of intracellular NO content was determined as earlier **(C)**. Results are the mean ± SEM of $n = 5$ independent experiments performed in triplicate, $^{*}p < 0.05$ or $^{**}p < 0.01$ relative to the respective vehicle group, $^{++}p < 0.01$ relative to the respective Ang-II-stimulated cells. In other experiments, cells were transfected with control siRNA **(D)**, RXRα-specific siRNA **(E)**, PPARα-specific siRNA **(F),** or PPARγ-specific siRNA **(G)** and stimulated with Ang-II (1 μM; 4 h) at 44 h post-transfection. In some experiments, cells were pretreated with Rosu (10 n*M*) plus Bex (0.3 μM) 20 h before Ang-II challenge and quantification of NO bioavailability was determined. Results are the mean ± SEM of $n = 5$ independent experiments performed in triplicate, $^{**}p < 0.01$ relative to the respective vehicle group, $^{++}p < 0.01$ relative to the respective Ang-II-stimulated cells.

significant efficacy when assessed individually. To further confirm this striking observation *in vivo,* daily Rosu administration at a dose four-fold-lower than that required to reduce atherosclerotic lesion formation (27), or Bex at a dose that was previously not found to inhibit acute TNFα-induced arteriolar leukocyte adhesion (55), was tested individually or in combination in mice subjected to chronic Ang-II infusion (56). In this model of systemic inflammation, arteriolar leukocyte adhesion remained unaltered in Rosu or Bex-treated animals, whereas combined administration of both drugs provoked a synergistic inhibitory effect. Furthermore, atheroma formation and MC infiltration in apoE$^{-/-}$ mice subjected to a high-fat diet was clearly diminished in animals treated with the drug combination, thus validating our *in vitro* observations in a relevant *in vivo* model.

Leukocyte/arterial interactions require both the expression of several types of CAMs in the endothelium and leukocytes as well as the presence of counter receptor molecules in the leukocyte/endothelial cell (14, 31). In addition to adhesion molecules, chemokines also have the potential to recruit specific cell types and are involved in the regulation of leukocyte trafficking (14). The ability of Ang-II to increase the endothelial expression of E-selectin, ICAM-1, and VCAM-1 and also the production of a wide array of leukocyte-recruiting chemokines is well known (2, 36, 42, 46, 54, 60). Statins are reported to reduce both the inflammation-induced expression of these endothelial CAMs and the synthesis of numerous chemokines (24, 38). More recently, we have demonstrated decreased expression of E-selectin, ICAM-1, and VCAM-1 and a decrease in the synthesis of CXCL1 or CCL2 by the endothelium with RXR agonists in an inflammatory environment (55). Therefore, it was perhaps not surprising that pretreatment of HUAECs with an Rosu + Bex combination reduced both the expression of CAMs and the synthesis of different chemokines involved in the MC arrest evoked by Ang-II. Furthermore, in the *in vivo* setting, the combined administration of suboptimal doses of Rosu + Bex, in addition to attenuating the increased expression of arteriolar E-selectin, ICAM-1, VCAM-1, and fractalkine, and the elevated circulating levels of CXCL1, CCL2, and CCL5 induced by chronic Ang-II exposure also decreased Ang-II-induced CD11b upregulation on circulating monocytes but not on neutrophils. This exciting observation may also suggest that this treatment may result in improved vascular function without compromising other neutrophilic responses required in host defense.

Having established the action of Rosu + Bex on the aforementioned components of the canonical leukocyte recruitment cascade, we sought to determine their effect on some intracellular signaling cascades triggered by activation

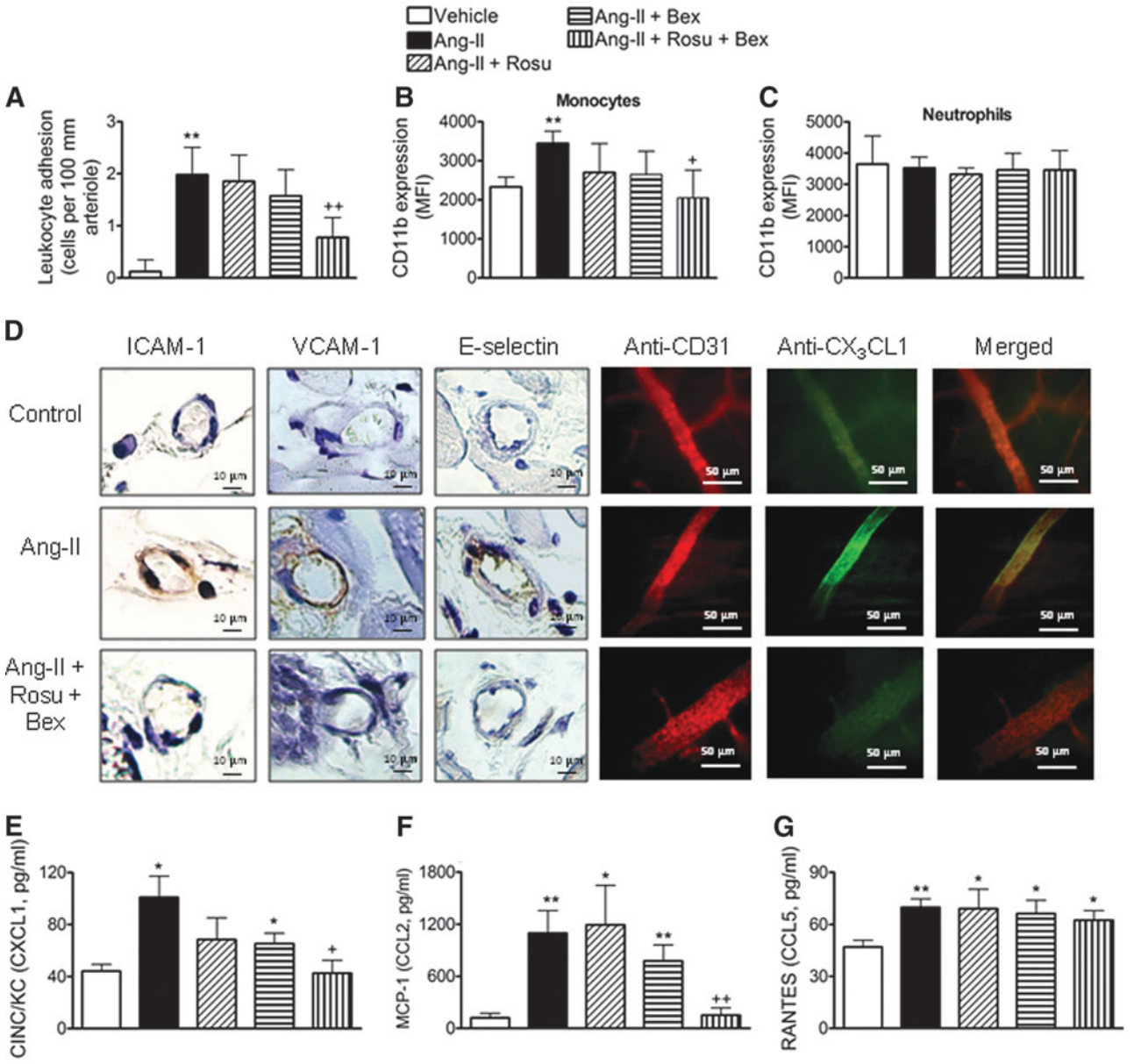

FIG. 9. ***In vivo*** **effects of suboptimal doses of Rosu+Bex.** Ang-II (500 ng/kg/min) or saline was delivered to mice using osmotic minipumps for 14 days. A group of Ang-II-infused mice was administered with Bex at 10 mg/kg/day by gavage or with Rosu at 1.25 mg/kg/day delivered through the osmotic minipump. An additional group of Ang-II chronically stimulated animals was treated with a combination of both compounds. Leukocyte adhesion to arterial endothelium was evaluated in the cremasteric microcirculation **(A)**. CD11b expression in heparinized whole blood was determined by flow cytometry on circulating monocytes and neutrophils **(B–C)**. ICAM-1, VCAM-1, E-selectin, and CX_3CL1 expression was determined by immunohistochemistry in the cremasteric arterioles. CD31 staining was used to distinguish vessels **(D)**. Circulating levels of CINC/KC **(E)**, MCP-1**(F),** and RANTES **(G)** were measured by ELISA in plasma samples. Results are the mean ± SEM of $n = 5$–6 independent experiments. $^{*}p < 0.05$ or $^{**}p < 0.01$ relative to vehicle-infused mice; $^{+}p < 0.05$ or $^{++}p < 0.05$ relative to the Ang-II-infused animals.

of the AT_1 Ang-II receptor. The RhoA-Rho kinase pathway has been implicated in leukocyte recruitment (4) and RhoA can be activated by Ang-II, as shown here and in a previous report (22). We show that targeted knockdown of RhoA in HUAECs diminished the adhesion of MCs triggered by Ang-II. Notably, Rosu + Bex abolished Ang-II-induced RhoA activation. Although blockade of the mevalonate pathway by statins can prevent the synthesis of isoprenoid intermediates, such as farnesyl pyrophosphate or geranylgeranyl pyrophosphate that are involved in the post-translational modification of numerous proteins including the γ subunit of heterotrimeric G proteins such as Rho (5, 19), the concentrations of statins required to inhibit Rho-kinase are much greater than those applied here (μM range *vs*. n*M*) (38, 51). Furthermore, to the best of our knowledge, the effect of Bex on RhoA activation has never been

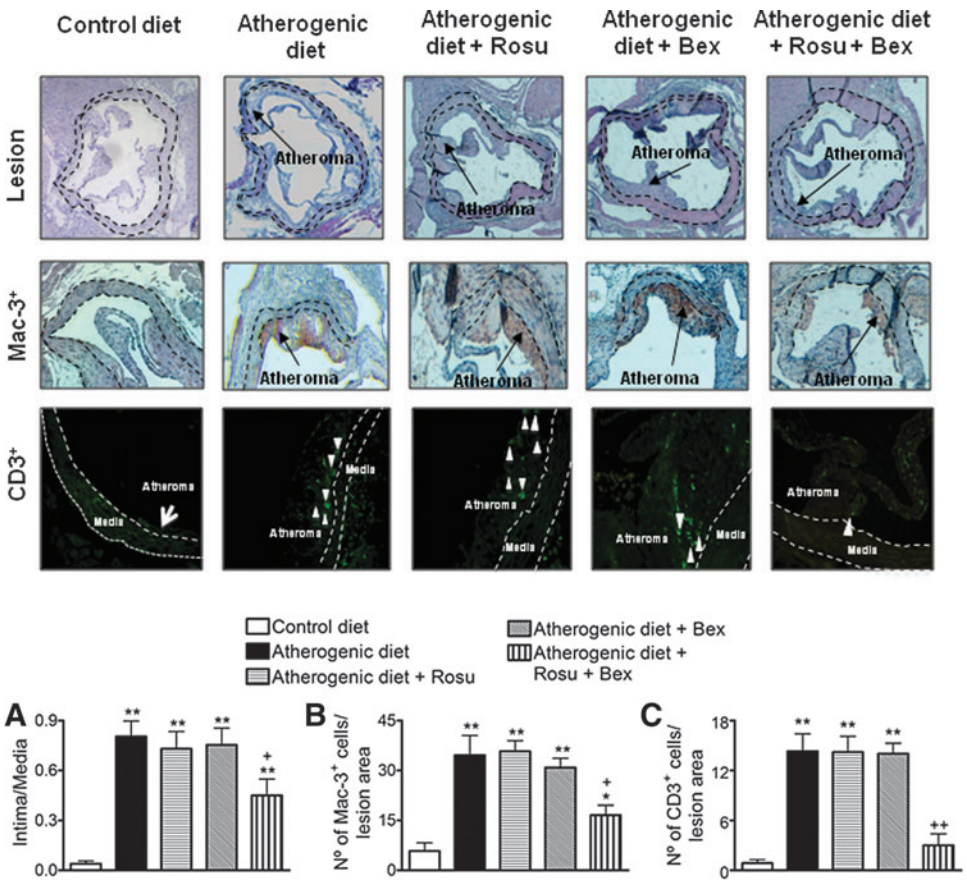

FIG. 10. Suboptimal doses of Rosu+Bex reduced atherosclerosis development and cell composition in apoE$^{-/-}$ mice on atherogenic diet. Mice were sacrificed at 16 weeks of age after 8 weeks on a low-fat standard diet (control diet), high-fat atherogenic diet (atherogenic diet), or high-fat atherogenic diet treated with Rosu (1.25 mg/kg/day delivered by osmotic minipumps), Bex (10 mg/kg/day) by gavage, or with a combination of both drugs. Atheroma lesion was determined in three to five histological sections per mice **(A)**. The discontinuous lines delineate the limits of the media. Macrophage (Mac-3$^+$, **B)** and T-cell (CD3$^+$, **C)** infiltration were also evaluated. Representative images of aortic root cross-sections, Mac-3$^+$ stained area (*brown staining*), and CD3$^+$ cells (*white arrowheads*) for the control or atherogenic diet-fed mice treated or not with the drugs are shown. *Black arrows* point to Mac-3$^+$ areas within the lesion. Results are the mean ± SEM of $n = 5$–7 animals per group. *$p < 0.05$ or **$p < 0.01$ relative to values animals subjected to a control diet; +$p < 0.05$ or ++$p < 0.01$ relative to values in untreated animals subjected to an atherogenic diet.

addressed. Therefore, additional studies were undertaken to address the inhibitory effect of Rosu + Bex on RhoA activation by Ang-II.

Guided by our initial observations, and given that RhoA is acknowledged as a primary target of oxidative stress on Ang-II endothelial stimulation (43), we explored the effect of the RXR agonist and statin combination on NADPH-oxidase-derived ROS production. Although Nox2, Nox4, and Nox5 are the most abundant NADPH oxidase isoforms in endothelial cells (29) and are induced by Ang-II (54), only Nox5 appears to play a major role in Ang-II-induced endothelial adhesiveness since both VCAM-1 and fractalkine upregulation and the subsequent MC arrest were found to be Nox5 mediated (39, 54). We found that Ang-II-induced production of ROS was attenuated by preincubation of HUAECs with Rosu + Bex. Moreover, Ang-II-dependent Nox2 and Nox5 expression was significantly reduced by the combined treatment and the former in murine aortic endothelial cells, which may account for the reduced arteriolar leukocyte adhesion encountered in animals subjected to chronic Ang-II infusion, as found in other animal models (11, 41). Furthermore, since mechanisms through which Ang-II-induced ROS production activate downstream signaling are elusive, we show here that RhoA activation is dependent on Nox5/NADPH oxidase activity. Conversely, knockdown of RhoA in HUAEC or its pharmacological inhibition affected neither Ang-II-induced ROS production nor the increase in Nox5 expression, indicating that ROS generation by Nox5 is an upstream regulator of RhoA activation in this experimental setting.

PPARs are ligand-activated nuclear hormone receptors that function as transcription factors. The three isoforms of PPAR (PPARα, PPARγ, and PPARβ/δ) are expressed in the endothelium and have been described to curb inflammation in atherosclerosis (3, 40). Ligand binding of PPAR promotes heterodimerization with the RXR receptor, inducing PPAR transactivation of target genes (40, 55). In this study, Rosu + Bex were found to enhance RXR, PPARα, and PPARγ protein expression in Ang-II-stimulated HUAECs.

Importantly, specific knockdown of endothelial RXR, PPARα, or PPARγ reversed the inhibitory effects exerted by Rosu + Bex on Ang-II-induced mononuclear leukocyte adhesion. Finally, a clear interaction between RXR/PPARα and RXR/PPARγ was revealed on co-incubation with Rosu and Bex at suboptimal concentrations. Considering that PPARα or PPARγ agonists can inhibit RhoA activation (45, 50) and exert antioxidant properties (40), it seems likely that inhibition of Nox5 expression and prevention of ROS generation inhibit RhoA activation *via* RXR/PPARα and RXR/PPARγ. Indeed, knockdown of RXRα, PPARα, or PPARγ abolished the inhibitory action of the drug combination on Ang-II-induced RhoA activation and Nox5 expression. In addition, RhoA has also been reported to be an upstream regulator of mitogen-activated protein kinase (MAPK) family members, such as p38 MAPK (33), and the latter can regulate the transcription of many genes through its action on downstream targets such as NF-κB (20, 53); both are involved in inflammatory responses such as the MC recruitment induced by Ang-II (54). Therefore, the inhibition of Ang-II-induced Nox5 activation and expression by Rosu + Bex combination may inhibit the activation of RhoA and different MAPKs that lead to activation of several transcription factors, including NFκB, and the further regulation of genes encoding different CAMs and chemokines, which actively participate in the mononuclear leukocyte recruitment induced by Ang-II (Supplementary Fig. S8).

Finally, Ang-II impairs endothelial function through superoxide anion generation and peroxynitrite formation, and eNOS inhibition and uncoupling, reducing NO bioavailability (32, 43), and the anti-adhesive properties of NO are widely recognized (17, 21). Here, we report that Ang-II stimulation reduced NO availability in HUAEC and this reduction was reversed by pretreatment with Rosu + Bex. In addition, silencing of Nox5 prevented the effects caused by Ang-II and, in the absence of RXRα, PPARα, or PPARγ, the combination of Rosu + Bex was unable to fully restore endothelial NO bioavailability. These results suggest that the effects achieved by the drug combination are mainly due to their antioxidant properties.

In conclusion, this study provides the first evidence that combined therapy with Rosu and Bex at suboptimal concentrations/doses exerts synergistic beneficial effects on endothelial dysfunction produced by Ang-II. This anti-inflammatory activity was found to be mediated through an Nox5-RhoA-RXR/PPAR-associated mechanism, linking redox-signaling pathways to MC recruitment.

Materials and Methods

Human in vitro *studies*

All investigation with human samples carried out in this study conforms to the principles outlined in the Declaration of Helsinki and was approved by the institutional ethics committee at the University Clinic Hospital of Valencia, Spain. Written informed consent was obtained from all volunteers.

Cell culture

HUAECs were isolated by collagenase treatment (26) and maintained in human endothelial cell basal medium-2 (EBM-2) supplemented with endothelial growth medium-2 (EGM-2) and 10% FCS. Cells at passage 1 were grown to confluence on 24-well culture plates. Before every experiment, cells were incubated for 16 h in medium containing 1% FCS and then returned to 10% FCS-supplemented medium at the commencement of all experimental protocols.

Leukocyte-HUAEC interactions under flow conditions

HUAECs at passage 1 were grown to confluence and stimulated with Ang-II (1 μM) for 4 h. Rosu (10–30 nM), Bex (0.3–1 μM), or combinations of both were added to plates 20 h before Ang-II stimulation. In another set of experiments, cells were incubated with the ROCK inhibitor Y27632 (10 μM) 1 h before Ang-II stimulation (1 μM, 4 h). Human MCs were obtained from buffy coats of healthy donors by Ficoll–Hypaque density gradient centrifugation (37). The Glycotech flow chamber was assembled and placed onto an inverted microscope stage, and freshly isolated human MCs (1×10^6/mL) were then perfused across the endothelial monolayers (HUAECs or transfected HUAECs). In all experiments, leukocyte interactions were determined after 5 min at 0.5 dyn/cm^2. Cells interacting on the surface of the endothelium were visualized and recorded ($\times$20 objective, $\times$10 eyepiece) using phase-contrast microscopy (Axio Observer A1; Carl Zeiss microscope).

Flow cytometry

Confluent endothelial cells were stimulated with Ang-II (1 μM) for 4 h (ICAM-1 and VCAM-1 expression) or 24 h (CX_3CL1 expression). In some experiments, cells were pretreated with Rosu (10 nM), Bex (0.3 μM), or a combination of Rosu (10 nM) plus Bex (0.3 μM) 20 h before Ang-II stimulation. Cells were detached, washed, and incubated at 2×10^6 cells/ml with a 1/100 dilution of primary antibodies against human VCAM-1 or ICAM-1 in PBS with 0.2% BSA and 0.05% NaN_3 for 1 h on ice. Detection of primary antibodies was performed using the appropriate Alexa Fluor 488-secondary antibody (dilution 1/250). For fractalkine expression, cells were incubated with a PE-conjugated mAb against human CX_3CL1 (1/25 dilution) for 1 h on ice in the same buffer. After two washes, cells were suspended in PBS containing 2% paraformaldehyde. The fluorescence signal of the labeled cells was then analyzed by flow cytometry (FACSVerse Flow Cytometer; BD Biosciences). The expression of ICAM-1, VCAM-1, and CX_3CL1 was expressed as the mean of fluorescence intensity (MFI).

Real time-polymerase chain reaction

Confluent HUAEC or murine endothelial cells were stimulated with Ang-II (1 μM) for 4 h. In some experiments, cells were pretreated with Rosu (10 nM), Bex (0.3 μM), or a combination of Rosu (10 nM) plus Bex (0.3 μM) 20 h before Ang-II stimulation. RNA from endothelial cells was obtained using Trizol Reagent, and purity and concentration was determined by the A260/280 ratio. RNA (500 ng) was reverse transcribed with the Maxima First-Strand cDNA Synthesis kit and amplified with Luminar Color HiGreen HigBox qPCR Master Mix. Reactions were run on a 7900 Fast Real-Time PCR System, and results were analyzed with the software provided

by the manufacturer (Applied Biosystems, Life Technologies). mRNA levels were determined following the $2^{-\Delta\Delta Ct}$ method using mouse *cyclophilin or human GAPDH* as an endogenous control and normalizing with regard to the control group. The following primers were designed with Primer Express software (Forward: Fw; Reverse: Rv): Human AT_1: Fw 5′ - ACGT GTCTCAGCATTGATCGAT-3′ and Rv 5′-TCGAAGGCGG GACTTCATT-3′ and human GAPDH: Fw 5′- ACCACAG TCCATGCCATCAC-3′ and Rv 5′-TCCACCACCCTGTTG CTGTA-3′. Mouse Cyclophilin Fw: 5′ TGGAGAGCACCAA GACAGACA-3′ and Rv 5′-TGCCGGAGTCGACAATGAT-3′; Mouse Nox 2: Fw 5′TCAAGACCATTGCAAGTGAAC AC-3′ and Rv 5′-TCAGGGCCACACAGGAAAA-3′: Mouse Nox 4: Fw5′- AGCATCTGCATCTGTCCTGAAC-3′ and .Rv 5′-ACTGTCCGGCACATAGGTAAAAG-3′: Mouse Duox 1: Fw 5′-AGCTCTCCGGGTCTGCAA-3′ and Rv 5′-CACATC TTCAGCCCTTTGTAGCTT-3′; Mouse Duox 2: Fw 5′-GAT CAGCATCAGACAGGGTTAGG-3′ and Rv 5′-TCTTCACG ACGCGCTTTCT-3′.

Immunofluorescence

Confluent endothelial cells were grown on glass coverslips and stimulated with Ang-II (1 μM) for 4 h (ICAM-1 and VCAM-1 expression) or 24 h (CX_3CL1 expression). In some experiments, cells were pretreated with Rosu (10 nM), Bex (0.3 μM), or a combination of Rosu (10 nM) plus Bex (0.3 μM) 20 h before Ang-II stimulation. The cells were fixed with 4% paraformaldehyde and blocked in a PBS solution containing 1% BSA. Next, they were incubated for 2 h with primary mouse antibodies against VCAM-1 or ICAM-1 (1/100 dilution), followed by a 45 min incubation at room temperature with an Alexa Fluor 488-conjugated goat anti-mouse secondary mAb (1/1000 dilution). For fractalkine detection, samples were incubated overnight with a primary mouse mAb against human CX_3CL1 (1:200 dilution) in a 0.1% BSA/PBS solution at 4°C. Cell nuclei were stained with 4′-6-diamidino-2-phenylindole (DAPI). Images were captured with an immunofluorescence microscope (Axio Observer A1; Carl Zeiss microscope).

Chemokine detection

Confluent endothelial cells were stimulated with Ang-II (1 μM) for 4 h. In some experiments, cells were pretreated with Rosu (10 nM), Bex (0.3 μM), or a combination of Rosu (10 nM) plus Bex (0.3 μM) 20 h before Ang-II stimulation. Human chemokines GROα (CXCL1), IL-8 (CXCL8), MCP-1 (CCL2), and RANTES (CCL5) were measured in HUAEC culture supernatants by ELISA. After coating the plates overnight with the primary antibody, nonspecific binding sites were blocked with 3% BSA for 1 h. Supernatants and standards were added to PBS/0.5% BSA/0.05% NaN_3 for 2 h. Biotinylated detector antibodies were added for 2 h, followed by neutravidin horseradish peroxidase for 1 h. All plate washes were carried out in four cycles in freshly prepared PBS/0.2% Tween 20. Enhanced K-Blue TMB substrate was added for 30 min, and the enzyme reaction was stopped by the addition of 0.19 M sulfuric acid. Absorbance was read at 450 nm, and the data were processed by GraphPad Prism software. Results are expressed as pM chemokine in the supernatant.

Gene knockdown by siRNA

Confluent HUAEC cultures were transfected with either control or Rho A, Nox 5, RXRα, PPARα, PPARβ, and PPARγ-specific siRNA using Lipofectamine RNAiMAX reagent. Protein expression was determined by immunoblot of cell lysates after 48 h and compared with the control siRNA to determine silencing efficiency.

Western blot and immunoprecipitation

After treatments, cells were washed, detached, collected, and centrifuged at 15,000 g at 4°C for 30 min. Protein content was determined according to Bradford's method. Samples were denatured, subjected to SDS-PAGE using a 10% running gel, and transferred to nitrocellulose membrane. Nonspecific binding sites were blocked with 3% BSA in TBS solution, and blots were incubated overnight with a mouse polyclonal antibody against human RhoA (dilution 1/250), a mouse polyclonal antibody against human Nox2 (0.2 μg/mL), a rabbit polyclonal antibody against human Nox4 (2 μg/ml), a rabbit polyclonal antibody against human Nox5 (dilution 1/500), a rabbit polyclonal antibody against human RXRα (dilution 1/500), a mouse polyclonal antibody against human PPARα (dilution 1/500), a rabbit polyclonal antibody against human PPARβ/δ (dilution 1/500), or a rabbit polyclonal antibody against human PPARγ (dilution 1/500). Subsequently, membranes were washed and incubated for 1 h with the corresponding secondary HRP-linked antibody and developed using the ECL procedure. Signals were detected using a luminescent reader (FujiFilm image Reader LAS1000; Fuji) and analyzed with ImageJ software (NIH, Windows free version).

For immunoprecipitation, cell extracts were prepared in 50 mM Tris-HCl (pH 8), 150 mM NaCl, 1% Nonidet P-40, with protease (1 mM PMSF, 40 μg/ml aprotinin, and 40 μg/ml leupeptin), and phosphatase (1 mM sodium ortovanadate and 1 mM NaF) inhibitors. Protein ($\sim$200 μg) from cell extracts was incubated with 5 μg of the rabbit polyclonal antibody against human PPARα or PPARγ. Immunocomplexes were precipitated using anti-rabbit IgG beads following the manufacturer's instructions and suspended in sample buffer containing freshly added 50 mM dithiothreitol (DTT). Immunoblotting was performed with an antibody against RXRα. Membranes were developed using horseradish peroxidase-conjugated rabbit TrueBlot as secondary antibody. Chemiluminescent signals were developed with ECL.

RhoA activation assay

HUAECs were grown to 70% confluence in six-well plates. Then, cells were left untransfected or transfected with a control siRNA or specific siRNA against Nox5, RXRα, PPARα, or PPARγ using Lipofectamine RNAiMAX. Twenty-four hours after transfection, cells were pretreated for 20 h with Rosu (10 nM), Bex (0.3 μM), or a combination of Rosu (10 nM) plus Bex (0.3 μM) before Ang-II stimulation (1 μM, 1 h) since Ang-II-induced RhoA activation peaks within the first hour of challenge (58). In additional assays, untransfected HUAECs were pretreated with the antioxidant apocynin (30 μM, 1 h) and subsequently stimulated with Ang-II (1 μM, 1 h). Then, cells were lysed, protein content was determined, and the RhoA activity was quantified using a commercial Rho G-LISA™assay kit.

NADPH oxidase activity assay

The activity of NADPH oxidase was measured in HUAECs by lucigenin-derived chemiluminiscence. HUAECs were pretreated for 20 h with Rosu (10 n*M*), Bex (0.3 μM), or a combination of Rosu (10 n*M*) plus Bex (0.3 μM) before Ang-II stimulation (1 μM, 1 h) since superoxide release induced by Ang-II is detected after 1 h challenge (10). In some experiments, cells were pretreated with the antioxidant apocynin (30 μM, 1 h) or with an RhoA inhibitor (C3 transferase, 2 μg/ml, 4 h) before Ang-II stimulation (1 μM, 1 h). After treatments, HUAECs were washed with ice-cold PBS, scraped, and centrifuged at 13,000 rpm for 1 min at 4°C. The resulting cell pellet was homogenized in lysis buffer (pH 7.0) containing 50 m*M* KH_2PO_4, 1 m*M* EGTA, and 150 m*M* sucrose at 4°C, and protein content was determined. Cellular extracts were incubated in PBS containing 5 μM lucigenin and 100 μM NADPH. Thereafter, luminiscence was measured every 10 s for 5 min in an Optocomp luminometer (MGM Instruments). The enzymatic activity was expressed as relative light units (RLU)/μg of protein/min.

Measurement of NO production in HUAEC

Intracellular NO was monitored with 4-amino-5-methylamino-2′,7′-difluorofluorescein diacetate (DAF-2-FM diacetate), a fluorescence indicator of NO that emits fluorescence in response to a reaction with NO, as previously described (47). To measure intracellular NO, HUAECs were seeded on 24-well plates. At 80% confluence, HUAECs were pretreated for 20 h with Rosu (10 n*M*), Bex (0.3 μM), or a combination of Rosu (10 n*M*) plus Bex (0.3 μM) and then stimulated with Ang-II (1 μM, 4 h). In another set of experiments, cells were pretreated with the antioxidant apocynin (30 μM, 1 h) or with an RhoA inhibitor (C3 transferase, 2 μg/ml, 4 h) before Ang-II stimulation (1 μM, 4 h). Finally, cells were transfected with a control siRNA or specific siRNAs against Nox5, RXRα, PPARα, or PPARγ. Twenty-four hours after transfection, HUAEC were pretreated for 20 h with or without Rosu (10 n*M*) plus Bex (0.3 μM) and then stimulated with Ang-II (1 μM, 4 h). After completion of the treatments, cells were loaded with 2.5 μM (DAF-2-FM diacetate) in EBM-2 supplemented with EGM-2 and 10% FCS for 30 min. After loading, cells were rinsed with PBS. To quantify the DAF-related fluorescence, cells were observed under an inverted fluorescence Nikon Eclipse Ti-S microscope. Fluorescence from five different fields per well was measured (excitation wavelength: 488 nm; emission wavelength: 515 nm). Fluorescence signals were quantified using NIS-Elements 3.2 software (Nikon Izasa S.A).

Animal studies

The animal protocol conforms to the Guide for the Care and Use of Laboratory Animals published by the US National Institutes of Health (NIH publication No. 85–23, revised 1996) and was approved by the Ethics Review Board of the School of Medicine, University of Valencia. Colonies of C57BL/6 mice (22–30 g, Charles River) were bred and maintained under specific pathogen-free conditions. For the entire experimental period, the mice were fed with an autoclaved balanced diet with free access to water.

Ang-II was administered to randomly selected groups of mice *via* subcutaneous osmotic minipumps set to deliver saline or Ang-II (500 ng/kg/min) for 14 days. This dose was selected based on its mild effects on blood pressure and clear leukocyte infiltration as previously described (56). A second group of mice were infused with Ang-II and administered by gavage with Bex (10 mg/kg/day); a third group was infused with Ang-II and Rosu (1.25 mg/kg/day delivered by osmotic minipumps); and a final Ang-II infused group was treated with a combination of both drugs.

Intravital microscopy

Mice were anesthetized by i.p. injection with a mixture of xylazine hydrochloride (10 mg/kg) and ketamine hydrochloride (200 mg/kg). The mouse cremasteric preparation used in this study was similar to that previously described (48). The cremaster muscle was dissected from the tissues and exteriorized on an optical clear viewing pedestal. The muscle was cut longitudinally with a cautery and held flat against the pedestal by attaching silk sutures to the corners of the tissue. The muscle was then perfused continuously with warmed bicarbonate-buffered saline (pH 7.4) at a rate of 1 ml/min. The cremasteric microcirculation was observed using an intravital microscope (Nikon Optiphot-2, SMZ1; Badhoevedorp) equipped with a 50× objective lens (Nikon SLDW; Badhoevedorp) and a 10×eyepiece. A video camera (Sony SSC-C350P; Koeln) mounted on the microscope projected the image onto a color monitor, and the images were CCD recorded for playback analysis. Cremasteric arterioles (20–40 μm in diameter) were selected for the study, and the diameter was measured online using a video caliper (Microcirculation Research Institute, Texas A&M University, College Station, TX). Centerline blood cell velocity was also measured online using an optical Doppler velocimeter (Microcirculation Research Institute). Vessel blood flow was calculated from the product of mean RBC velocity (Vmean = centerline blood cell velocity/1.6) and cross-sectional area, assuming cylindrical geometry. Wall shear rate (γ) was calculated based on the Newtonian definition: $\gamma = 8 \times (V_{mean}/D_v)\ s^{-1}$, in which D_v is vessel diameter (25).

The number of adherent leukocytes was determined offline during playback of videotaped images. A leukocyte was defined as adherent to arteriolar endothelium when it was stationary for at least 30 s. Leukocyte adhesion was expressed as the number per 100 μm length of vessel. In each animal, leukocyte responses were measured in three to five randomly selected arterioles. At the end of the experiments, animals were humanely euthanized by anesthetic overdose.

Whole mount immunohistochemistry

Once intravital microscopy determinations were performed, mice were sacrificed and the cremaster muscle was isolated and fixed in 4% paraformaldehyde for 10 minutes. The protocol followed was similar to that previously described (35); briefly, whole-mounted muscles were incubated for 2 h in 0.2% Triton X-100, 1% BSA, and 0.5% horse serum in PBS. They were then incubated overnight at 4°C with a primary antibody rabbit anti-mouse CX_3CL1 (1/100 dilution) or eFluor 450-conjugated anti-mouse CD31 (PECAM-1) (1/100 dilution). Samples were subsequently washed with PBS and incubated for 1.5 h at room temperature with Alexa Fluor

488-conjugated donkey anti-rabbit secondary antibody (1/500 dilution). All antibodies were diluted in 0.1% PBS/BSA. The muscles were then mounted with Slowfade Gold Reagent. Images were acquired with a fluorescence microscope (Axio Observer A1) equipped with a 40× objective lens and a 10× eyepiece.

Immunohistochemistry

After completion of the intravital microscopy measurements, the cremaster muscle was isolated and fixed in 4% paraformaldehyde, dehydrated using a graded acetone series at 4°C, and embedded in paraffin wax for assessment of ICAM-1, VCAM-1, and E-selectin as previously described (55). Tissue sections (5 μm) were incubated against mouse ICAM-1, VCAM-1, and E-selectin (all dilutions 1:50) overnight at 4°C and then for a further 60 min at 37°C with a biotinylated anti-rabbit secondary antibody (1:500 dilution), streptavidin-HRP, and diaminobenzidine substrate. Slides were counterstained with hematoxylin. Positive staining was defined as an arteriole displaying a brown reaction product.

Determination of CD11b integrin expression by flow cytometry

Heparinized whole blood samples were stained for 30 min with saturated amounts (1:10 dilution) of PE-conjugated anti-CD115 antibody, VH-450-conjugated anti-Ly6G antibody, and APC-conjugated anti-CD11b antibody. Red blood cells were lysed using a commercial lysing solution, and samples were run in a flow cytometer (FACSVerse Flow Cytometer; BD Biosciences). The expression of CD11b (CFS fluorescence) in monocytes and neutrophils was measured according to the expression of CD115 and Ly6G, respectively, and expressed as the MFI.

Plasma chemokine detection

KC (CXCL1), MCP-1 (CCL2), and RANTES (CCL5) in mice plasma samples were measured using commercial ELISA kits. The OD values were recorded on a microplate reader at 450 nm. The concentrations of cytokines in samples were calculated from a standard curve generated using recombinant chemokines.

Measurement of glucose and lipid profile

Circulating glucose and lipid levels in plasma of mice fasted overnight were measured using enzymatic procedures (WAKO) and the Ascensia Elite glucometer (Bayer HealthCare).

Measurement of blood pressure

Systolic blood pressure was measured in conscious mice using a noninvasive tail cuff system with a photoelectric sensor (Niprem 645; Cibertec S.A) using a Niprem 1.8 software (Cibertec S.A.). During the procedure, animals were placed in the restrainer tube of a chamber that was kept at 36°C (LE5002 Pressure Meter; PANLAB) as previously described (62). Mice were acclimated to the instrument for 5 continuous days before baseline measurements and then daily for the remainder 14 days. Blood pressure measurements were determined every day. Each data are the average of 10 values recorded for each animal and used for analysis.

In an additional group of experiments, Ang-II 1000 ng/kg/min was administered *via* subcutaneous osmotic minipumps for 14 days. A second group of mice were infused with Ang-II and administered by gavage with Bex (10 mg/kg/day); a third group was infused with Ang-II and Rosu (1.25 mg/kg/day delivered by osmotic minipumps); and a final Ang-II-infused group was treated with a combination of both drugs.

Evaluation of diet-induced atherosclerosis

ApoE$^{-/-}$ (C57BL/6J) female mice were obtained from Charles River laboratories and kept on a low-fat standard diet (2.8% fat). At 8 weeks of age, mice were fed with a high-fat atherogenic diet (10.8% total fat, 0.75% cholesterol) for 8 weeks alone (atherogenic diet group) or treated with Bex (10 mg/kg/day) by gavage, Rosu (1.25 mg/kg/day delivered by osmotic minipumps), or a combination of both drugs. The control mouse group was maintained on a low-fat standard diet for 8 weeks. After treatments, hearts containing the aortic root were removed from mice, washed with PBS, fixed with 4% paraformaldehyde/PBS overnight, and paraffin embedded for sectioning and analysis, as described (54).

Atherosclerosis was evaluated in at least three to five aortic root cross-sections stained with hematoxylin/eosin (16). Lesion size was quantified as the intima-to-media ratio in cross-sections of paraffin-embedded aortic root. For macrophage quantification in lesions, a rat anti-Mac-3 monoclonal antibody (1/200 dilution) was used. After peroxidase inactivation (H_2O_2, 0.3%) and blockade with horse serum, samples were incubated overnight (4°C) with the primary antibody. Detection was performed with a biotin-conjugated goat anti-rat secondary antibody (1/300 dilution) followed by HRP-streptavidin and DAB substrate incubation. Slides were counterstained with hematoxylin and mounted with EU-KITT. For T-cell detection within the lesion, aortic root cross-sections were blocked as described earlier, incubated overnight with an anti-CD3 antibody (1/75 dilution) followed by an incubation for 1 h at room temperature with an Alexa Fluor 488-conjugated goat anti-rabbit secondary antibody, and mounted with Slow-Fade Gold antifade reagent. Preparations were analyzed by fluorescent microscopy with an inverted fluorescent microscope (Axio Observer A1).

Additional materials

Ang-II was purchased from Calbiochem. Bex, and Rosu were obtained from Axxora (BioVision). Endothelial basal medium-2 (EMB-2), EGM-2, and FCS were purchased from Lonza Iberica. Ketamine and xylazine hydrochloride were supplied by ORION Pharma. Apocynin, mouse anti-human β-actin mAb (clone AC-15), and anti-Nox5 C-terminal polyclonal antibody produced in rabbit that detects the 86 kDa band, hematoxylin, and Y27632 were purchased from Sigma-Aldrich. Nevertheless, there are other antibodies in the literature that can detect a 70 kDa band of Nox5 (39). The rabbit polyclonal against mouse CX_3CL1, the PE-conjugated rat monoclonal against mouse CD31 (clone 390), and TrueBlot Anti-Rabbit Ig IP beads were provided by eBioscience. The PE-conjugated mouse monoclonal against human CX_3CL1 (clone 51637), primary mouse monoclonal mAb against human CX_3CL1 (clone 81506), primary chicken mAb against mouse E-selectin, human GRO-α, IL-8, MCP-1, and RANTES

antibody pairs were purchased from R&D Systems. The mouse monoclonal anti-human RhoA Ab, rabbit polyclonal anti-human Nox4, the rabbit polyclonal anti-human PPARα Ab, the rabbit polyclonal anti-human PPARβ/δ Ab, and the rabbit polyclonal anti-human PPARγ Ab were supplied by Abcam. The primary mouse mAb against human VCAM-1, the primary mouse mAb against human ICAM-1, the mouse monoclonal anti-human Nox2 (clone NL7) Ab, and the DAB substrate was purchased from Serotec. Sodium heparin (5000 U/ml or 50 mg/ml) was supplied by Pharmaceutical Laboratories Rovi SA. Ficoll-Paque TM PLUS and ECL developer were purchased from GE Healthcare. DAPI, DAF-2-FM diacetate and Alexa Fluor 488-conjugated secondary antibodies were from Molecular Probes-Invitrogen. The secondary Abs, HRP-linked anti-goat, HRP-linked anti-rabbit, HRP-linked anti-mouse, and the anti-mouse CD3 antibody were purchased from Dako. HRP-Streptavidin was from LABVISION Corporation. The RhoA-specific siRNA and Ultra TMB-ELISA were purchased from Thermo Fisher Scientific, Inc. Nox5, RXRα, PPARα, PPARβ/δ, and PPARγ-specific siRNA were purchased from Dharmacon. The Alzet 2004 osmotic minipumps, C57BL/6 and ApoE$^{-/-}$ mice were from Charles River. The primary rabbit mAb against mouse VCAM-1, primary rabbit mAb against mouse ICAM-1, the PE-conjugated mAb against mouse CD115 (clone AF598), the VH-450-conjugated mAb against mouse Ly6G (clone 1A8) and APC-conjugated mAb against mouse CD11b (clone M1/70), and the lysing solution were from BD Pharmingen. The biotinylated anti-rabbit secondary Ab, rabbit polyclonal against PPARγ, rabbit polyclonal against RXRα, mouse monoclonal against PPARα, the anti-Mac-3 mAb (clone M3/84), and the biotin-conjugated goat anti-rat secondary Ab were purchased from Santa Cruz Biotechnology. The EUKITT was provided by Deltalab. The G-LISA RhoA activation assay Biochem kit and cell-permeable C3 transferase (RhoA inhibitor) were from Cytoskeleton, Inc. Slowfade Gold Reagent and lipofectamine RNAiMAX were from Invitrogen. The mouse RANTES ELISA kit was for RayBiotech. Recombinant human GRO-α, IL-8, MCP-1, and RANTES were acquired from Peprotech. Murine aortic endothelial cells were from Innoprot. Maxima First-Strand cDNA Synthesis kit and Luminar Color HiGreen HigBox qPCR Master Mix were from Fermentas, Thermo Fisher Scientific. The low-fat standard diet was from Panlab. The high-fat atherogenic diet (10.8% total fat, 0.75% cholesterol) was acquired from Sniff.

Statistical analysis

Values were expressed as mean ± SEM. Differences between two groups were determined by paired or unpaired Student's *t* test, as appropriate. Data within multiple groups were compared using an analysis of variance (one-way ANOVA), including a Newman–Keuls *post hoc* test for multiple comparisons. Data were considered statistically significant when $p < 0.05$.

Acknowledgments

This study was supported by grants SAF2011-23777, CPII13/00025, PI012/01271, CP10/00555, and PI13/00834 from the Spanish Ministry of Economy and Competiveness, Carlos III Health Institute, Spanish Ministry of Health, the European Regional Development Fund (FEDER), and research grants from Generalitat Valenciana (GVACOMP2014-006 and PROMETEO II/2013/014). PE is a recipient of a predoctoral grant (FPU) from the Spanish Ministry of Education. The technical assistance of Virginia López is greatly acknowledged. A part of these results were presented at the 19th World Congress on Heart Disease and the XXXV Congress of the Spanish Society of Pharmacology in 2014.

Author Disclosure Statement

The authors have no conflicting financial interests.

References

1. Alberts AW. Discovery, biochemistry and biology of lovastatin. *Am J Cardiol* 62: 10J–15J, 1988.
2. Alvarez A, Cerda-Nicolas M, Naim Abu Nabah Y, Mata M, Issekutz AC, Panes J, Lobb RR, and Sanz MJ. Direct evidence of leukocyte adhesion in arterioles by angiotensin II. *Blood* 104: 402–408, 2004.
3. Balakumar P and Mahadevan N. Interplay between statins and PPARs in improving cardiovascular outcomes: a double-edged sword? *Br J Pharmacol* 165: 373–379, 2012.
4. Cernuda-Morollon E and Ridley AJ. Rho GTPases and leukocyte adhesion receptor expression and function in endothelial cells. *Circ Res* 98: 757–767, 2006.
5. Cordle A, Koenigsknecht-Talboo J, Wilkinson B, Limpert A, and Landreth G. Mechanisms of statin-mediated inhibition of small G-protein function. *J Biol Chem* 280: 34202–34209, 2005.
6. Desjardins F, Sekkali B, Verreth W, Pelat M, De Keyzer D, Mertens A, Smith G, Herregods MC, Holvoet P, and Balligand JL. Rosuvastatin increases vascular endothelial PPARgamma expression and corrects blood pressure variability in obese dyslipidaemic mice. *Eur Heart J* 29: 128–137, 2008.
7. de Vries-van der Weij J, de Haan W, Hu L, Kuif M, Oei HL, van der Hoorn JW, Havekes LM, Princen HM, Romijn JA, Smit JW, and Rensen PC. Bexarotene induces dyslipidemia by increased very low-density lipoprotein production and cholesteryl ester transfer protein-mediated reduction of high-density lipoprotein. *Endocrinology* 150: 2368–2375, 2009.
8. Dormuth CR, Hemmelgarn BR, Paterson JM, James MT, Teare GF, Raymond CB, Lafrance JP, Levy A, Garg AX, and Ernst P. Use of high potency statins and rates of admission for acute kidney injury: multicenter, retrospective observational analysis of administrative databases. *BMJ* 346: f880, 2013.
9. Dzau VJ. Theodore Cooper Lecture: tissue angiotensin and pathobiology of vascular disease: a unifying hypothesis. *Hypertension* 37: 1047–1052, 2001.
10. Estelles R, Milian L, Nabah YN, Mateo T, Cerda-Nicolas M, Losada M, Ivorra MD, Issekutz AC, Cortijo J, Morcillo EJ, Blazquez MA, and Sanz MJ. Effect of boldine, secoboldine, and boldine methine on angiotensin II-induced neutrophil recruitment *in vivo*. *J Leukoc Biol* 78: 696–704, 2005.
11. Fan LM, Douglas G, Bendall JK, McNeill E, Crabtree MJ, Hale AB, Mai A, Li JM, McAteer MA, Schneider JE, Choudhury RP, and Channon KM. Endothelial cell-specific reactive oxygen species production increases susceptibility to aortic dissection. *Circulation* 129: 2661–2672, 2014.
12. Farol LT and Hymes KB. Bexarotene: a clinical review. *Expert Rev Anticancer Ther* 4: 180–188, 2004.

13. Florentin M, Liberopoulos EN, Rizos CV, Kei AA, Liamis G, Kostapanos MS, and Elisaf MS. Colesevelam plus rosuvastatin 5 mg/day versus rosuvastatin 10 mg/day alone on markers of insulin resistance in patients with hypercholesterolemia and impaired fasting glucose. *Metab Syndr Relat Disord* 11: 152–156, 2013.
14. Galkina E and Ley K. Immune and inflammatory mechanisms of atherosclerosis (*). *Annu Rev Immunol* 27: 165–197, 2009.
15. Golomb BA and Evans MA. Statin adverse effects: a review of the literature and evidence for a mitochondrial mechanism. *Am J Cardiovasc Drugs* 8: 373–418, 2008.
16. Gonzalez-Navarro H, Abu Nabah YN, Vinue A, Andres-Manzano MJ, Collado M, Serrano M, and Andres V. p19(ARF) deficiency reduces macrophage and vascular smooth muscle cell apoptosis and aggravates atherosclerosis. *J Am Coll Cardiol* 55: 2258–2268, 2010.
17. Granger DN and Kubes P. Nitric oxide as antiinflammatory agent. *Methods Enzymol* 269: 434–442, 1996.
18. Granger DN, Vowinkel T, and Petnehazy T. Modulation of the inflammatory response in cardiovascular disease. *Hypertension* 43: 924–931, 2004.
19. Greenwood J, Steinman L, and Zamvil SS. Statin therapy and autoimmune disease: from protein prenylation to immunomodulation. *Nat Rev Immunol* 6: 358–370, 2006.
20. Guo RW, Yang LX, Li MQ, Liu B, and Wang XM. Angiotensin II induces NF-kappa B activation in HUVEC via the p38MAPK pathway. *Peptides* 27: 3269–3275, 2006.
21. Hickey MJ and Kubes P. Role of nitric oxide in regulation of leucocyte-endothelial cell interactions. *Exp Physiol* 82: 339–348, 1997.
22. Higuchi S, Ohtsu H, Suzuki H, Shirai H, Frank GD, and Eguchi S. Angiotensin II signal transduction through the AT1 receptor: novel insights into mechanisms and pathophysiology. *Clin Sci (Lond)* 112: 417–428, 2007.
23. Hoffman KB, Kraus C, Dimbil M, and Golomb BA. A survey of the FDA's AERS database regarding muscle and tendon adverse events linked to the statin drug class. *PLoS One* 7: e42866, 2012.
24. Hot A, Lavocat F, Lenief V, and Miossec P. Simvastatin inhibits the pro-inflammatory and pro-thrombotic effects of IL-17 and TNF-alpha on endothelial cells. *Ann Rheum Dis* 72: 754–760, 2013.
25. House SD and Lipowsky HH. Leukocyte-endothelium adhesion: microhemodynamics in mesentery of the cat. *Microvasc Res* 34: 363–379, 1987.
26. Jaffe EA, Nachman RL, Becker CG, and Minick CR. Culture of human endothelial cells derived from umbilical veins. Identification by morphologic and immunologic criteria. *J Clin Invest* 52: 2745–2756, 1973.
27. Kleemann R, Princen HM, Emeis JJ, Jukema JW, Fontijn RD, Horrevoets AJ, Kooistra T, and Havekes LM. Rosuvastatin reduces atherosclerosis development beyond and independent of its plasma cholesterol-lowering effect in APOE*3-Leiden transgenic mice: evidence for antiinflammatory effects of rosuvastatin. *Circulation* 108: 1368–1374, 2003.
28. Landmesser U, Hornig B, and Drexler H. Endothelial function: a critical determinant in atherosclerosis? *Circulation* 109: II27–II33, 2004.
29. Lassegue B and Griendling KK. NADPH oxidases: functions and pathologies in the vasculature. *Arterioscler Thromb Vasc Biol* 30: 653–661, 2010.
30. Laursen JB, Rajagopalan S, Galis Z, Tarpey M, Freeman BA, and Harrison DG. Role of superoxide in angiotensin II-induced but not catecholamine-induced hypertension. *Circulation* 95: 588–593, 1997.
31. Libby P. Inflammation in atherosclerosis. *Nature* 420: 868–874, 2002.
32. Loot AE, Schreiber JG, Fisslthaler B, and Fleming I. Angiotensin II impairs endothelial function via tyrosine phosphorylation of the endothelial nitric oxide synthase. *J Exp Med* 206: 2889–2896, 2009.
33. Marinissen MJ, Chiariello M, Tanos T, Bernard O, Narumiya S, and Gutkind JS. The small GTP-binding protein RhoA regulates c-jun by a ROCK-JNK signaling axis. *Mol Cell* 14: 29–41, 2004.
34. Marinou K, Tousoulis D, Antonopoulos AS, Stefanadi E, and Stefanadis C. Obesity and cardiovascular disease: from pathophysiology to risk stratification. *Int J Cardiol* 138: 3–8, 2010.
35. Massena S, Christoffersson G, Hjertstrom E, Zcharia E, Vlodavsky I, Ausmees N, Rolny C, Li JP, and Phillipson M. A chemotactic gradient sequestered on endothelial heparan sulfate induces directional intraluminal crawling of neutrophils. *Blood* 116: 1924–1931, 2010.
36. Mateo T, Abu Nabah YN, Abu Taha M, Mata M, Cerda-Nicolas M, Proudfoot AE, Stahl RA, Issekutz AC, Cortijo J, Morcillo EJ, Jose PJ, and Sanz MJ. Angiotensin II-induced mononuclear leukocyte interactions with arteriolar and venular endothelium are mediated by the release of different CC chemokines. *J Immunol* 176: 5577–5586, 2006.
37. Mateo T, Naim Abu Nabah Y, Losada M, Estelles R, Company C, Bedrina B, Cerda-Nicolas JM, Poole S, Jose PJ, Cortijo J, Morcillo EJ, and Sanz MJ. A critical role for TNFalpha in the selective attachment of mononuclear leukocytes to angiotensin-II-stimulated arterioles. *Blood* 110: 1895–1902, 2007.
38. Mira E and Manes S. Immunomodulatory and anti-inflammatory activities of statins. *Endocr Metab Immune Disord Drug Targets* 9: 237–247, 2009.
39. Montezano AC, Burger D, Paravicini TM, Chignalia AZ, Yusuf H, Almasri M, He Y, Callera GE, He G, Krause KH, Lambeth D, Quinn MT, and Touyz RM. Nicotinamide adenine dinucleotide phosphate reduced oxidase 5 (Nox5) regulation by angiotensin II and endothelin-1 is mediated via calcium/calmodulin-dependent, rac-1-independent pathways in human endothelial cells. *Circ Res* 106: 1363–1373, 2010.
40. Moraes LA, Piqueras L, and Bishop-Bailey D. Peroxisome proliferator-activated receptors and inflammation. *Pharmacol Ther* 110: 371–385, 2006.
41. Murdoch CE, Chaubey S, Zeng L, Yu B, Ivetic A, Walker SJ, Vanhoutte D, Heymans S, Grieve DJ, Cave AC, Brewer AC, Zhang M, and Shah AM. Endothelial NADPH oxidase-2 promotes interstitial cardiac fibrosis and diastolic dysfunction through proinflammatory effects and endothelial-mesenchymal transition. *J Am Coll Cardiol* 63: 2734–2741, 2014.
42. Nabah YN, Mateo T, Estelles R, Mata M, Zagorski J, Sarau H, Cortijo J, Morcillo EJ, Jose PJ, and Sanz MJ. Angiotensin II induces neutrophil accumulation *in vivo* through generation and release of CXC chemokines. *Circulation* 110: 3581–3586, 2004.
43. Nguyen Dinh Cat A, Montezano AC, Burger D, and Touyz RM. Angiotensin II, NADPH oxidase, and redox signaling

in the vasculature. *Antioxid Redox Signal* 19: 1110–1120, 2013.
44. Nickenig G and Murphy TJ. Enhanced angiotensin receptor type 1 mRNA degradation and induction of polyribosomal mRNA binding proteins by angiotensin II in vascular smooth muscle cells. *Mol Pharmacol* 50: 743–751, 1996.
45. Paintlia AS, Paintlia MK, Singh AK, and Singh I. Modulation of Rho-Rock signaling pathway protects oligodendrocytes against cytokine toxicity via PPAR-alpha-dependent mechanism. *Glia* 61: 1500–1517, 2013.
46. Pastore L, Tessitore A, Martinotti S, Toniato E, Alesse E, Bravi MC, Ferri C, Desideri G, Gulino A, and Santucci A. Angiotensin II stimulates intercellular adhesion molecule-1 (ICAM-1) expression by human vascular endothelial cells and increases soluble ICAM-1 release *in vivo*. *Circulation* 100: 1646–1652, 1999.
47. Peiro C, Vallejo S, Gembardt F, Palacios E, Novella S, Azcutia V, Rodriguez-Manas L, Hermenegildo C, Sanchez-Ferrer CF, and Walther T. Complete blockade of the vasorelaxant effects of angiotensin-(1–7) and bradykinin in murine microvessels by antagonists of the receptor Mas. *J Physiol* 591(Pt 9): 2275–2285, 2013.
48. Piqueras L, Sanz MJ, Perretti M, Morcillo E, Norling L, Mitchell JA, Li Y, and Bishop-Bailey D. Activation of PPARbeta/delta inhibits leukocyte recruitment, cell adhesion molecule expression, and chemokine release. *J Leukoc Biol* 86: 115–122, 2009.
49. Plutzky J. The PPAR-RXR transcriptional complex in the vasculature: energy in the balance. *Circ Res* 108: 1002–1016.
50. Ramirez SH, Heilman D, Morsey B, Potula R, Haorah J, and Persidsky Y. Activation of peroxisome proliferator-activated receptor gamma (PPARgamma) suppresses Rho GTPases in human brain microvascular endothelial cells and inhibits adhesion and transendothelial migration of HIV-1 infected monocytes. *J Immunol* 180: 1854–1865, 2008.
51. Rashid M, Tawara S, Fukumoto Y, Seto M, Yano K, and Shimokawa H. Importance of Rac1 signaling pathway inhibition in the pleiotropic effects of HMG-CoA reductase inhibitors. *Circ J* 73: 361–370, 2009.
52. Ridker PM, Danielson E, Fonseca FA, Genest J, Gotto AM, Jr., Kastelein JJ, Koenig W, Libby P, Lorenzatti AJ, MacFadyen JG, Nordestgaard BG, Shepherd J, Willerson JT, and Glynn RJ. Rosuvastatin to prevent vascular events in men and women with elevated C-reactive protein. *N Engl J Med* 359: 2195–2207, 2008.
53. Rius C, Abu-Taha M, Hermenegildo C, Piqueras L, Cerda-Nicolas JM, Issekutz AC, Estan L, Cortijo J, Morcillo EJ, Orallo F, and Sanz MJ. Trans- but not cis-resveratrol impairs angiotensin-II-mediated vascular inflammation through inhibition of NF-kappaB activation and peroxisome proliferator-activated receptor-gamma upregulation. *J Immunol* 185: 3718–3727, 2010.
54. Rius C, Piqueras L, Gonzalez-Navarro H, Albertos F, Company C, Lopez-Gines C, Ludwig A, Blanes JI, Morcillo EJ, and Sanz MJ. Arterial and venous endothelia display differential functional fractalkine (CX3CL1) expression by angiotensin-II. *Arterioscler Thromb Vasc Biol* 33: 96–104, 2013.
55. Sanz MJ, Albertos F, Otero E, Juez M, Morcillo EJ, and Piqueras L. Retinoid X receptor agonists impair arterial mononuclear cell recruitment through peroxisome proliferator-activated receptor-gamma activation. *J Immunol* 189: 411–424, 2012.
56. Scalia R, Gong Y, Berzins B, Freund B, Feather D, Landesberg G, and Mishra G. A novel role for calpain in the endothelial dysfunction induced by activation of angiotensin II type 1 receptor signaling. *Circ Res* 108: 1102–1111, 2011.
57. Scarisbrick JJ, Morris S, Azurdia R, Illidge T, Parry E, Graham-Brown R, Cowan R, Gallop-Evans E, Wachsmuth R, Eagle M, Wierzbicki AS, Soran H, Whittaker S, and Wain EM. U.K. consensus statement on safe clinical prescribing of bexarotene for patients with cutaneous T-cell lymphoma. *Br J Dermatol* 168: 192–200, 2013.
58. Shatanawi A, Romero MJ, Iddings JA, Chandra S, Umapathy NS, Verin AD, Caldwell RB, and Caldwell RW. Angiotensin II-induced vascular endothelial dysfunction through RhoA/Rho kinase/p38 mitogen-activated protein kinase/arginase pathway. *Am J Physiol Cell Physiol* 300: C1181–C1192, 2011.
59. Stalker TJ, Lefer AM, and Scalia R. A new HMG-CoA reductase inhibitor, rosuvastatin, exerts anti-inflammatory effects on the microvascular endothelium: the role of mevalonic acid. *Br J Pharmacol* 133: 406–412, 2001.
60. Tummala PE, Chen XL, Sundell CL, Laursen JB, Hammes CP, Alexander RW, Harrison DG, and Medford RM. Angiotensin II induces vascular cell adhesion molecule-1 expression in rat vasculature: a potential link between the renin-angiotensin system and atherosclerosis. *Circulation* 100: 1223–1229, 1999.
61. Vakeva L, Ranki A, and Hahtola S. Ten-year experience of bexarotene therapy for cutaneous T-cell lymphoma in Finland. *Acta Derm Venereol* 92: 258–263, 2012.
62. Zhang Y, Naggar JC, Welzig CM, Beasley D, Moulton KS, Park HJ, and Galper JB. Simvastatin inhibits angiotensin II-induced abdominal aortic aneurysm formation in apolipoprotein E-knockout mice: possible role of ERK. *Arterioscler Thromb Vasc Biol* 29: 1764–1771, 2009.

Address correspondence to:
Dr. Maria-Jesus Sanz
Institute of Health Research INCLIVA
University Clinic Hospital of Valencia
Av. Menéndez Pelayo 4
Valencia 46010
Spain

E-mail: maria.j.sanz@uv.es

Dr. Laura Piqueras
Institute of Health Research INCLIVA
University Clinic Hospital of Valencia
Av. Menéndez Pelayo 4
Valencia 46010
Spain

E-mail: piqueras_lau@gva.es

Date of first submission to ARS Central, April 28, 2014; date of final revised submission, January 2, 2015; date of acceptance, January 19, 2015.

Abbreviations Used

Ang-II = angiotensin II
Bex = bexarotene
CAM = cell adhesion molecule
DAPI = 4′-6-diamidino-2-phenylindole
EBM-2 = endothelial cell basal medium-2
EGM-2 = endothelial growth medium-2
ELISA = enzyme-linked immunoassay
eNOS = endothelial nitric oxide synthase
GROα = growth regulated oncogene-α
HUAEC = human umbilical artery endothelial cells
ICAM-1 = intercellular adhesion molecule-1
IL-8 = interleukin-8
MAPK = mitogen-activated protein kinase
MC = mononuclear cell
MCP-1 = monocyte chemotactic protein-1
MFI = mean fluorescence intensity
PPAR = peroxisome proliferator-activated receptor
RANTES = regulated on activation, normal T cell expressed and secreted
ROCK = Rho-associated protein kinase
ROS = reactive oxygen species
Rosu = rosuvastatin
RXR = retinoid X receptor
siRNA = small interfering RNA
TNFα = tumor necrosis factor-α
VCAM-1 = vascular cell adhesion molecule-